Journal of the Mechanics and Physics of Solids 61 (2013) 19–37

Contents lists available at SciVerse ScienceDirect

Journal of the Mechanics and Physics of Solids

journal homepage: www.elsevier.com/locate/jmps

The nonlinear elastic response of suspensions of rigid inclusions in rubber: II—A simple explicit approximation for finite-concentration suspensions

Oscar Lopez-Pamies [a,*], Taha Goudarzi [a], Kostas Danas [b]

[a] Department of Civil and Environmental Engineering, University of Illinois, Urbana-Champaign, IL 61801-2352, USA
[b] Laboratoire de Mécanique des Solides, C.N.R.S. UMR7649, École Polytechnique, ParisTech, 91128 Palaiseau Cedex, France

ARTICLE INFO

Article history:
Received 18 June 2012
Received in revised form
20 August 2012
Accepted 24 August 2012
Available online 6 September 2012

Keywords:
Finite strain
Hydrodynamic reinforcement
Iterated dilute homogenization
Comparison medium methods

ABSTRACT

In Part I, an exact solution was determined for the problem of the overall nonlinear elastic response of Gaussian (or Neo-Hookean) rubber reinforced by a dilute isotropic distribution of rigid particles. Here, this fundamental result is utilized to construct an approximate solution for non-Gaussian rubber reinforced by an isotropic distribution of rigid particles at finite concentration. This is accomplished by means of two different techniques in two successive steps. First, the dilute solution is utilized together with a differential scheme in finite elasticity to generate a solution for Neo-Hookean rubber filled with an isotropic distribution of rigid particles of polydisperse sizes and finite concentration. This non-dilute result is then employed within the context of a new comparison medium method — derived as an extension of Talbot-Willis (1985) variational framework to the non-convex realm of finite elasticity — to generate in turn a corresponding solution for filled non-Gaussian rubber wherein the underlying elastomeric matrix is characterized by any I_1-based stored-energy function $\Psi(I_1)$ of choice. The solution is fully explicit and remarkably simple. Its key theoretical and practical merits are discussed in detail.

Additionally, the constructed analytical solution is confronted to 3D finite-element simulations of the large-deformation response of Neo-Hookean and non-Gaussian rubber reinforced by isotropic distributions of rigid spherical particles with the same size, as well as with different sizes. Good agreement is found among all three sets of results. The implications of this agreement are discussed.

1. Introduction

In the preceding paper (Lopez-Pamies et al., in press), henceforth referred to as Part I, we determined an exact solution for the overall (or macroscopic) nonlinear elastic response of Gaussian (or Neo-Hookean) rubber reinforced by a dilute isotropic distribution of rigid particles. The objective of this paper is to make use of this fundamental result to construct an approximate solution for the corresponding response of *non-Gaussian* rubber reinforced by an isotropic distribution of rigid particles at *finite concentration*. Given that standard reinforcing fillers (e.g., carbon black and silica) typically agglomerate into "particles" of many different sizes (see, e.g., Chapter 4 in Leblanc, 2010 and references therein), the focus is in particular on

* Corresponding author. Tel.: +1 2172441242; fax: +1 2172658039.
E-mail addresses: pamies@illinois.edu (O. Lopez-Pamies), goudarz2@illinois.edu (T. Goudarzi), kdanas@lms.polytechnique.fr (K. Danas).

0022-5096/$ - see front matter © 2012 Elsevier Ltd. All rights reserved.
http://dx.doi.org/10.1016/j.jmps.2012.08.013

isotropic distributions of particles of polydisperse sizes. This is accomplished here with the help of two different techniques in two successive steps. In the first step of the derivation, the dilute solution of Part I is extended to finite-concentration suspensions of particles in Neo-Hookean rubber via an iterated dilute homogenization technique. In the second step, a nonlinear comparison medium technique is utilized to construct in turn an approximate solution[1] for finite-concentration suspensions of particles in non-Gaussian rubber.

Iterated dilute homogenization methods—also referred to as differential schemes—are a class of iterative techniques that make use of results for the overall properties of dilute composites in order to generate corresponding results for composites with finite concentration of constituents. The basic form of these techniques was introduced in the 1930s by Bruggeman (1935) to determine the linear dielectric constant and conductivity of a certain class of two-phase composites. The idea was later generalized by various authors to determine the *linear* mechanical/physical properties of multiphase composites with an admittedly broad range of microstructures; see, e.g., Norris (1985), Avellaneda (1987), Braides and Lukkassen (2000), and Chapter 10.7 in the monograph by Milton (2002). To be useful, these techniques require knowledge of a dilute solution from which to start the iterative construction process. It is because of this requirement that this approach has been utilized by and large in the restricted context of linear problems where — as opposed to nonlinear problems — there is a wide variety of dilute solutions available. Nevertheless, the central idea of these techniques is geometrical in nature and can therefore be applied to any constitutively *nonlinear* problem of choice, provided, again, the availability of a relevant dilute solution. In the context of finite elasticity of interest in this work, Lopez-Pamies (2010a) has recently put forward an iterated dilute homogenization technique for the special case of two-phase composites. In this paper, we utilize this technique together with the dilute solution of Part I in order to construct a solution for the nonlinear elastic response of Neo-Hookean rubber reinforced by an isotropic distribution of polydisperse rigid particles at finite concentration.

Comparison medium methods are variational techniques that allow to generate approximations for the overall properties of composites in terms of the properties of "simpler" comparison media. The idea behind these techniques was formalized for *linear* problems by Hashin and Shtrikman (1962) and later recognized by Willis (1983) to be apposite to deal with *nonlinear* problems as well. In a seminal contribution, Talbot and Willis (1985) provided a fairly general framework for constructing approximations for the overall nonlinear mechanical/physical properties of composites in terms of the overall properties of any comparison medium of choice, possibly nonlinear and heterogeneous. To render useful approximations, however, this framework requires the selection of an "optimal" comparison medium complex enough to mimic the behavior of the actual nonlinear composite yet simple enough that its overall properties can be computed. In the context of finite elasticity, such a selection process has proved particularly challenging because of the *constitutive non-convexity* and *nonlinear incompressibility constraint* typical of nonlinear elastic solids. Among the various attempts that have been pursued (Ponte Castañeda, 1989; Ponte Castañeda and Tiberio, 2000), the latest choice of a comparison medium that is a *linear composite* as prescribed by Lopez-Pamies and Ponte Castañeda (2006) has led to the more physically consistent results thus far. Yet, a critical limitation of this approach is that it cannot rigorously recover the overall incompressibility constraint typical of filled elastomers beyond 2D problems (Lahellec et al., 2004; Lopez-Pamies, 2008). In this paper, we work out an extension of the framework of Talbot and Willis (1985) that is free of the limitations of previous formulations at the expense of employing a *nonlinear composite* as the comparison medium. With the filled Neo-Hookean rubber constructed from the above-described iterated dilute homogenization technique as the choice for the comparison medium, we then employ this new formulation to generate an explicit approximate solution for the nonlinear elastic response of isotropic suspensions of rigid particles of polydisperse sizes and finite concentration in non-Gaussian rubber.

For purposes of gaining further insight and of assessing the accuracy of the proposed analytical approximation, in this paper we also generate full 3D FE (finite-element) results for the large-deformation response of Neo-Hookean and non-Gaussian rubber reinforced by isotropic distributions of rigid spherical particles. Specifically, we consider the cases of infinite periodic media where the repeated unit cells contain a large number of monodisperse and polydisperse spherical particles that are randomly distributed as dictated by a sequential adsorption algorithm. Full 3D computations of this sort have been previously considered in the context of infinitesimal elasticity by a number of authors (see, e.g., Gusev, 1997; Michel et al., 1999; Segurado and Llorca, 2002; Galli et al., 2008), but the finite elasticity simulations performed in this paper appear to be the first of their kind in the literature.

The presentation of the work is organized as follows. Section 2 introduces some basic notation and formulates the problem of the overall response of non-Gaussian rubber reinforced by a random and isotropic distribution of rigid particles under arbitrarily large deformations. In Section 3, the iterated dilute homogenization technique is presented and utilized together with the dilute solution of Part I to derive the first main result of this paper: *the overall nonlinear elastic response of Neo-Hookean rubber with stored-energy function $W=\mu/2[I_1-3]$, filled with an isotropic distribution of rigid particles of polydisperse sizes and finite concentration c, is characterized by the effective stored-energy function*

$$\overline{W}=\frac{\mu}{2(1-c)^{5/2}}[\overline{I}_1-3]. \tag{1}$$

[1] As in Part I, this work concentrates on the "hydrodynamic" reinforcing effect of the fillers and thus filled elastomers are viewed as two-phase particulate composites comprising a continuous nonlinear elastic matrix phase reinforced by a statistically uniform distribution of firmly bonded rigid inclusions.

Here, μ stands for the initial shear modulus of the rubber and $\bar{I}_1 = \overline{\mathbf{F}} \cdot \overline{\mathbf{F}}$ is the first principal invariant associated with the macroscopic deformation gradient $\overline{\mathbf{F}}$. The extension of the Talbot–Willis framework to finite elasticity for the case when the comparison medium is selected as a nonlinear composite is worked out in Section 4. In that same section, the framework is employed with the Neo-Hookean result (1) as the choice for the comparison medium in order to derive the following more general result: *the overall nonlinear elastic response of non-Gaussian rubber with I_1-based stored-energy function $W = \Psi(I_1)$, filled with an isotropic distribution of rigid particles of polydisperse sizes and finite concentration c, is characterized by the effective stored-energy function*

$$\overline{W} = (1-c)\Psi\left(\frac{\bar{I}_1 - 3}{(1-c)^{7/2}} + 3\right). \tag{2}$$

Section 4 includes a discussion of the key theoretical and practical merits of this result. The FE calculations are presented in Section 5, and compared with the analytical solution (2) in Section 6. Finally, Section 7 provides some concluding remarks.

2. The problem

The general problem to be addressed is that of determining the overall (or macroscopic) elastic response of an elastomer reinforced by a random distribution of rigid particles firmly bonded across interfaces that is subjected to arbitrarily large deformations. The spatial distribution of the particles is taken to be statistically uniform and their sizes to be much smaller than the macroscopic size. The constitutive behavior of the elastomer is characterized by a quasi-convex stored-energy function W of the deformation gradient $\mathbf{F}$. The rigid particles are also described as nonlinear elastic solids with stored-energy function

$$W_p(\mathbf{F}) = \begin{cases} 0 & \text{if} \quad \mathbf{F} = \mathbf{Q} \in Orth^+ \\ +\infty & \text{otherwise} \end{cases}, \tag{3}$$

where $Orth^+$ stands for the set of all proper orthogonal second-order tensors. The Lagrangian pointwise constitutive relation for the material is thus formally given by

$$\mathbf{S} = \frac{\partial W}{\partial \mathbf{F}}(\mathbf{X},\mathbf{F}), \quad W(\mathbf{X},\mathbf{F}) = (1-\theta(\mathbf{X}))W(\mathbf{F}) + \theta(\mathbf{X})W_p(\mathbf{F}), \tag{4}$$

where $\mathbf{S}$ denotes the first Piola–Kirchhoff stress tensor and θ is the indicator function of the spatial regions occupied collectively by the particles, taking the value of 1 if the position vector $\mathbf{X}$ lies in a particle and zero otherwise.

The filled elastomer is considered to occupy a domain Ω, with boundary $\partial\Omega$, in its undeformed stress-free configuration and, for convenience, units of length are chosen so that Ω has unit volume. The regions occupied by the elastomer and particles are respectively denoted by Ω_m and Ω_p so that $\Omega = \Omega_m \cup \Omega_p$. The macroscopic response of the material can then be defined as the relation between the averages of the first Piola–Kirchhoff stress $\mathbf{S}$ and the deformation gradient $\mathbf{F}$ over the volume Ω under the affine displacement boundary condition $\mathbf{x} = \overline{\mathbf{F}}\mathbf{X}$ on $\partial\Omega$, where the second-order tensor $\overline{\mathbf{F}}$ is a prescribed quantity (Hill, 1972). In this case, it follows from the divergence theorem that $\int_\Omega \mathbf{F}(\mathbf{X})\, d\mathbf{X} = \overline{\mathbf{F}}$, and hence the derivation of the macroscopic response reduces to finding the average stress $\overline{\mathbf{S}} \doteq \int_\Omega \mathbf{S}(\mathbf{X})\, d\mathbf{X}$ for a given $\overline{\mathbf{F}}$. The result reads formally as

$$\overline{\mathbf{S}} = \frac{\partial \overline{W}}{\partial \overline{\mathbf{F}}}(\overline{\mathbf{F}},c), \tag{5}$$

with

$$\overline{W}(\overline{\mathbf{F}},c) = (1-c)\min_{\mathbf{F}\in\mathcal{K}} \frac{1}{|\Omega_m|}\int_{\Omega_m} W(\mathbf{F})\, d\mathbf{X}. \tag{6}$$

In these last expressions, $\overline{W}$ is the so-called effective stored-energy function (which physically corresponds to the total elastic energy per unit undeformed volume stored in the material), $c \doteq \int_\Omega \theta(\mathbf{X})\, d\mathbf{X}$ is the initial volume fraction or concentration of particles, and $\mathcal{K}$ denotes a suitable set of kinematically admissible deformation gradient fields with prescribed volume average $\overline{\mathbf{F}}$.

2.1. The case of isotropic suspensions in non-Gaussian rubber

The main objective of this work is to determine the effective stored-energy function (6) for the practically relevant case when the particles are polydisperse in size and isotropically distributed in space, and the elastomeric matrix is isotropic and incompressible. The focus is on elastomers characterized by I_1-based stored-energy functions

$$W(\mathbf{F}) = \begin{cases} \Psi(I_1) & \text{if} \quad J \doteq \lambda_1\lambda_2\lambda_3 = 1, \\ +\infty & \text{otherwise}, \end{cases} \tag{7}$$

where $I_1=\mathbf{F}\cdot\mathbf{F}=\lambda_1^2+\lambda_2^2+\lambda_3^2$, λ_1, λ_2, λ_3 have been introduced to denote the singular values of the deformation gradient $\mathbf{F}$, and Ψ is any non-negative function of choice satisfying the linearization conditions

$$\Psi(3)=0 \quad \text{and} \quad \frac{\mathrm{d}\Psi}{\mathrm{d}I_1}(3)=\frac{\mu}{2}, \tag{8}$$

with μ denoting the initial shear modulus of the elastomeric matrix, and the physically based strong ellipticity conditions (Zee and Sternberg, 1983)

$$\frac{\mathrm{d}\Psi}{\mathrm{d}I_1}(I_1)>0 \quad \text{and} \quad \frac{\mathrm{d}\Psi}{\mathrm{d}I_1}(I_1)+2[I_1-\lambda_k^2-2\lambda_k^{-1}]\frac{\mathrm{d}^2\Psi}{\mathrm{d}I_1^2}(I_1)>0 \quad (k=1,2,3) \quad \forall\, I_1\geq 3. \tag{9}$$

Stored-energy functions of the functional form (7) with (8)–(9) are generalizations of the classical Neo-Hookean energy $\Psi(I_1)=\mu/2[I_1-3]$ that have been shown to describe reasonably well the response of a wide variety of elastomers over large ranges of deformations (see, e.g., Arruda and Boyce, 1993; Gent, 1996; Lopez-Pamies, 2010b). These types of constitutive models have the further merit that they are derivable from microscopic considerations based on realistic non-Gaussian statistical distributions of the underlying polymeric chains (see, e.g., Beatty, 2003).

Owing to the assumed isotropy of the microstructure and the constitutive isotropy and incompressibility of the matrix material (7) and rigid particles (3), the resulting overall elastic response is isotropic and incompressible. This implies that the effective stored-energy function $\overline{W}$ in this case depends on the macroscopic deformation gradient $\overline{\mathbf{F}}$ only through its singular values $\overline{\lambda}_1$, $\overline{\lambda}_2$, $\overline{\lambda}_3$ and becomes unbounded for non-isochoric deformations when $\overline{J}\doteq\det\overline{\mathbf{F}}=\overline{\lambda}_1\overline{\lambda}_2\overline{\lambda}_3\neq 1$. Accordingly, the result (6) can be simply written as a symmetric function of $\overline{\lambda}_1$, $\overline{\lambda}_2$, $\overline{\lambda}_3$ subject to the constraint $\overline{\lambda}_1\overline{\lambda}_2\overline{\lambda}_3=1$. Alternatively, in this work we shall find it more convenient to write (6) as a function solely of the two principal invariants $\overline{I}_1=\overline{\mathbf{F}}\cdot\overline{\mathbf{F}}=\overline{\lambda}_1^2+\overline{\lambda}_2^2+\overline{\lambda}_3^2$ and $\overline{I}_2=\overline{\mathbf{F}}^{-T}\cdot\overline{\mathbf{F}}^{-T}=\overline{\lambda}_1^2\overline{\lambda}_2^2+\overline{\lambda}_1^2\overline{\lambda}_3^2+\overline{\lambda}_2^2\overline{\lambda}_3^2$ in the form

$$\overline{W}(\overline{\mathbf{F}},c)=\begin{cases}\overline{\Psi}(\overline{I}_1,\overline{I}_2,c) & \text{if } \overline{J}=\overline{\lambda}_1\overline{\lambda}_2\overline{\lambda}_3=1,\\ +\infty & \text{otherwise.}\end{cases} \tag{10}$$

As outlined in the Introduction, our strategy to generate a solution for (10) involves two main steps and makes use of two different techniques. In the first step, presented in Section 3, we work out a solution for the special case of filled Neo-Hookean rubber by means of an iterated dilute homogenization technique. This Neo-Hookean solution is then utilized in the second step, presented in Section 4, to work out in turn a solution for filled non-Gaussian rubber via a nonlinear comparison medium method. In order to assist the presentation of the results, the unbounded branch of the energies (7) and (10) is omitted in most of the remainder of the analysis.

3. A solution for filled Neo-Hookean rubber via iterated dilute homogenization

In this section, we construct a solution for the effective stored-energy function (10) for the special case when the elastomeric matrix is Neo-Hookean rubber. This amounts to solving the relevant minimization problem (6) with (7) and

$$\Psi(I_1)=\frac{\mu}{2}[I_1-3]. \tag{11}$$

To this end, we make use of the iterated dilute homogenization procedure of Lopez-Pamies (2010a) together with the result derived in Part I as the required dilute solution from which we start the iterative construction process. For clarity of exposition, we first present the iterated dilute homogenization technique in its general form (Section 3.1) and then work out its application to filled Neo-Hookean rubber (Section 3.2).

3.1. An iterated dilute homogenization method in finite elasticity

Following Lopez-Pamies (2010a), we begin by considering that the unit-volume domain Ω is occupied by matrix material 0, a homogeneous elastomer with stored-energy function W (possibly compressible and anisotropic at this stage). We then embed a *dilute* distribution of rigid particles (of possibly any shape and orientation) with infinitesimal concentration ϕ_1 in material 0 in such a way that the total volume of the composite remains unaltered at $|\Omega|=1$; that is, we remove a total volume ϕ_1 of material 0 and replace it with rigid particles. Assuming a polynomial asymptotic behavior in ϕ_1, the resulting reinforced material has an effective stored-energy function $\overline{W}_1$ of the form

$$\overline{W}_1(\overline{\mathbf{F}},\phi_1)=W(\overline{\mathbf{F}})+\mathcal{G}\{W(\overline{\mathbf{F}});\overline{\mathbf{F}}\}\phi_1+O(\phi_1^2), \tag{12}$$

where $\mathcal{G}$ is a functional with respect to its first argument W and a function with respect to its second argument $\overline{\mathbf{F}}$.

Considering next $\overline{W}_1$ as the stored-energy function of a "homogeneous" matrix material 1, we repeat the same process of removal and replacing while keeping the volume fixed at $|\Omega|=1$. This second iteration requires utilizing rigid particles that are much larger in size than those used in the first iteration, since the matrix material 1 with stored-energy function (12) is being considered as homogeneous. Specifically, we remove an infinitesimal volume ϕ_2 of matrix material 1 and

replace it with rigid particles. The composite has now an effective stored-energy function

$$\overline{W}_2(\overline{\mathbf{F}},c_2)=\overline{W}_1(\overline{\mathbf{F}},\phi_1)+\mathcal{G}\{\overline{W}_1(\overline{\mathbf{F}},\phi_1);\overline{\mathbf{F}}\}\phi_2, \tag{13}$$

where the order of the asymptotic correction term has been omitted for notational simplicity. We remark that the functional $\mathcal{G}$ in (13) is the same as in (12) because we are considering *exactly the same* dilute distribution as in (12). More elaborate construction processes are possible (corresponding, for instance, to using different particle shapes and orientations at each iteration), but such a degree of generality is not needed for our purposes here. We further remark that the total concentration of rigid particles at this stage is given by $c_2=\phi_2+\phi_1(1-\phi_2)=1-\prod_{j=1}^{2}(1-\phi_j)$, and hence that the increment in total concentration of rigid particles in this second iteration is given by $c_2-\phi_1=\phi_2(1-\phi_1)$.

It is apparent now that repeating the same above process $i+1$ times, where i is an arbitrarily large integer, generates a particle-reinforced nonlinear elastic solid with effective stored-energy function

$$\overline{W}_{i+1}(\overline{\mathbf{F}},c_{i+1})=\overline{W}_i(\overline{\mathbf{F}},c_i)+\mathcal{G}\{\overline{W}_i(\overline{\mathbf{F}},c_i);\overline{\mathbf{F}}\}\phi_{i+1}, \tag{14}$$

which contains a *total* concentration of rigid particles given by

$$c_{i+1}=1-\prod_{j=1}^{i+1}(1-\phi_j). \tag{15}$$

For unbounded i the right-hand side of expression (15) is, roughly speaking, the sum of infinitely many concentrations of infinitesimal value, which can amount to a total concentration c_{i+1} of *finite* value. The increment in total concentration of rigid particles in this iteration (i.e., in passing from i to $i+1$) reads as

$$c_{i+1}-c_i=\prod_{j=1}^{i}(1-\phi_j)-\prod_{j=1}^{i+1}(1-\phi_j)=\phi_{i+1}(1-c_i), \tag{16}$$

from which it is a trivial matter to establish the following identity:

$$\phi_{i+1}=\frac{c_{i+1}-c_i}{1-c_i}. \tag{17}$$

Substituting expression (17) in (14) renders

$$(1-c_i)\frac{\overline{W}_{i+1}(\overline{\mathbf{F}},c_{i+1})-\overline{W}_i(\overline{\mathbf{F}},c_i)}{c_{i+1}-c_i}-\mathcal{G}\{\overline{W}_i(\overline{\mathbf{F}},c_i);\overline{\mathbf{F}}\}=0. \tag{18}$$

This difference equation can be finally recast — upon using the facts that the increment $c_{i+1}-c_i$ is infinitesimally small and that i is arbitrarily large — as the following initial value problem:

$$(1-c)\frac{\partial\overline{W}}{\partial c}(\overline{\mathbf{F}},c)-\mathcal{G}\{\overline{W}(\overline{\mathbf{F}},c);\overline{\mathbf{F}}\}=0,\quad \overline{W}(\overline{\mathbf{F}},0)=W(\overline{\mathbf{F}}). \tag{19}$$

The differential equation $(19)_1$, subject to the initial condition $(19)_2$, provides an implicit framework for constructing solutions for the effective stored-energy function $\overline{W}$ of elastomers reinforced by *finite concentrations* c of rigid particles directly in terms of corresponding solutions — as characterized by the functional $\mathcal{G}$ — when the particles are present in dilute concentration. It is worthwhile to emphasize that the formulation (19) is applicable to any choice of the stored-energy function W (including compressible and anisotropic) describing the behavior of the underlying elastomeric matrix. By construction, the results generated from (19) correspond to polydisperse microstructures where the particles have infinitely many diverse sizes. Again, this feature is of practical relevance here because standard reinforcing fillers (e.g., carbon black and silica) typically agglomerate, resulting effectively in polydisperse microstructures with "particles" of many different sizes. By the same token, the results generated from (19) are *realizable* in the sense that they are exact for a given class of microstructures. This implies that the generated effective stored-energy functions $\overline{W}$ are theoretically and physically sound. They are then guaranteed, for instance, to be objective in $\overline{\mathbf{F}}$, to linearize properly, and to comply with any macroscopic constraints imposed by microscopic constraints, such as the strongly nonlinear constraint of incompressibility. To be useful, however, the formulation (19) requires having knowledge of the functional $\mathcal{G}$ describing the relevant dilute response of the filled elastomer of interest, which is in general a notable challenge.

3.2. Application to filled Neo-Hookean rubber

In Part I, with help of the realizable homogenization theory developed in Lopez-Pamies et al. (2011), we derived a solution for the overall nonlinear elastic response of Neo-Hookean rubber reinforced by a dilute isotropic distribution of rigid particles. Below, we make direct use of this result in the framework (19) to construct in turn a corresponding solution for Neo-Hookean rubber reinforced by an isotropic distribution of rigid particles with polydisperse sizes at *finite concentration*.

The exact form of the solution derived in Part I is given implicitly in terms of an Eikonal partial differential equation in two variables which ultimately needs to be solved numerically (see Eqs. (42) and (37)–(38) in Part I). To make analytical progress, we do not utilize here the exact form of the solution but instead invoke its closed-form approximation, as devised

in Section 6 of Part I. In terms of the notation introduced in (10)–(12), this approximate dilute solution takes the form

$$\overline{\Psi}(\bar{I}_1,\bar{I}_2,c)=\Psi(\bar{I}_1)+\mathcal{G}\{\Psi(\bar{I}_1);\bar{I}_1,\bar{I}_2\}c, \tag{20}$$

where c is the infinitesimal concentration of particles, $\Psi(\bar{I}_1)=\mu/2[\bar{I}_1-3]$, and the functional $\mathcal{G}$ is given explicitly by

$$\mathcal{G}\{\Psi(\bar{I}_1);\bar{I}_1,\bar{I}_2\}=\frac{5}{2}\Psi(\bar{I}_1). \tag{21}$$

Substitution of (21) in the general formulation (19) leads to the initial-value problem

$$(1-c)\frac{\partial\overline{\Psi}}{\partial c}(\bar{I}_1,\bar{I}_2,c)-\frac{5}{2}\overline{\Psi}(\bar{I}_1,\bar{I}_2,c)=0,\quad \overline{\Psi}(\bar{I}_1,\bar{I}_2,0)=\Psi(\bar{I}_1)=\frac{\mu}{2}[\bar{I}_1-3], \tag{22}$$

which defines the effective stored-energy function $\overline{\Psi}$ of Neo-Hookean rubber filled with an isotropic distribution of rigid particles of polydisperse sizes and finite concentration c. Remarkably, this first-order partial differential equation admits the explicit solution

$$\overline{\Psi}(\bar{I}_1,\bar{I}_2,c)=\frac{\mu}{2(1-c)^{5/2}}[\bar{I}_1-3]. \tag{23}$$

Thorough comments on the theoretical and practical merits of this result are deferred to Section 4.2, where the more general case of filled non-Gaussian rubber is addressed. At this stage it is important to emphasize, however, that the effective stored-energy function (23) is not in general an exact realizable result. This is because use has been made of the approximate functional (21) — and *not* the exact functional — in the formulation (19) in order to favor analytical tractability. Nevertheless, in view of the high functional and quantitative accuracy of the approximation (21) for the dilute response (see Section 6 in Part I), the stored-energy function (23) is expected to be very close to an exact realizable result.[2]

4. A solution for filled non-Gaussian rubber via a nonlinear comparison medium method

The general case of isotropic suspensions of rigid particles in non-Gaussian rubber could be addressed by means of the same iterated dilute homogenization technique utilized in the foregoing section for Neo-Hookean rubber. That route would require explicit knowledge of the appropriate functional $\mathcal{G}$ in (19), which in principle could be computed by means of the same procedure followed in Part I but now specialized to energies of the form (7) as opposed to just the Neo-Hookean energy (11). While plausible, preliminary calculations indicate that this approach is not likely to provide explicit results and hence we do not pursue it here.

In the sequel, stimulated by the works of Willis (1994), Talbot and Willis (1994), and deBotton and Shmuel (2010), we pursue instead a nonlinear comparison medium approach. Roughly speaking, the idea is to make use of the formalism of Talbot and Willis (1985) to devise a variational framework that allows to construct an explicit approximate solution for the effective stored-energy function (10) for filled non-Gaussian rubber directly in terms of the "simpler" effective stored-energy function (23) for filled Neo-Hookean rubber. We begin in Section 4.1 by presenting the comparison medium framework in its general form and then work out its application to filled non-Gaussian rubber in Section 4.2.

4.1. A nonlinear comparison medium method in finite elasticity

In order to account for the perfectly rigid behavior (3) of the particles in the analysis that follows, it is expedient not to work with (3) directly but to consider instead the regularized case of *compressible non-rigid* particles with stored-energy function

$$W_p(\mathbf{F})=f_p(\mathbf{F},J)=\frac{\mu_p}{2}[\mathbf{F}\cdot\mathbf{F}-3]+\mu_p\left[\frac{1}{2}(J-1)^2-(J-1)\right], \tag{24}$$

where the material parameter μ_p denotes the initial shear modulus of the particles and the notation $W_p(\mathbf{F})=f_p(\mathbf{F},J)$ has been introduced for subsequent use; the special case of rigid behavior (3) can then be readily recovered from (24) by taking the limit $\mu_p\to+\infty$. Also for subsequent use, the stored-energy function for the elastomeric matrix material is rewritten here in the form

$$W(\mathbf{F})=f_m(\mathbf{F},J). \tag{25}$$

Consistent with the notation introduced in (24) and (25), we henceforth rewrite the pointwise energy (4) for the filled elastomer as

$$W(\mathbf{X},\mathbf{F})=f(\mathbf{X},\mathbf{F},J)=(1-\theta(\mathbf{X}))f_m(\mathbf{F},J)+\theta(\mathbf{X})f_p(\mathbf{F},J). \tag{26}$$

Now, borrowing ideas from Talbot and Willis (1985), it proves fruitful to introduce a comparison medium with pointwise energy

$$W_0(\mathbf{X},\mathbf{F})=f_0(\mathbf{X},\mathbf{F},J), \tag{27}$$

[2] In this regard, it is interesting to recall that the analogous solution $\overline{\Psi}=\mu/(2(1-c)^2)[\bar{I}_1-2]$ for the corresponding 2D problem is an exact realizable result (Lopez-Pamies, 2010a).

where f_0 is at this stage an arbitrary function, and to define the Legendre transformation[3]

$$(f-f_0)^*(\mathbf{X},\mathbf{P},Q) \doteq \sup_{\mathbf{F},\,J}[\mathbf{P}\cdot\mathbf{F}+Q\,J-f(\mathbf{X},\mathbf{F},J)+f_0(\mathbf{X},\mathbf{F},J)]. \tag{28}$$

Note that while the function $(f-f_0)$ may not be convex in $\mathbf{F}$ and J, the function $(f-f_0)^*$ is convex in $\mathbf{P}$ and Q by definition.

A direct consequence from (28) is that, for any $\mathbf{P}$, Q, $\mathbf{F}$, and J,

$$W(\mathbf{X},\mathbf{F}) = f(\mathbf{X},\mathbf{F},J) \geq f_0(\mathbf{X},\mathbf{F},J)+\mathbf{P}\cdot\mathbf{F}+Q\,J-(f-f_0)^*(\mathbf{X},\mathbf{P},Q), \tag{29}$$

and hence that

$$\overline{W}(\overline{\mathbf{F}},c) \geq \min_{\mathbf{F}\in\mathcal{K}} \int_\Omega [f_0(\mathbf{X},\mathbf{F},J)+\mathbf{P}\cdot\mathbf{F}+Q\,J]\mathrm{d}\mathbf{X} - \int_\Omega (f-f_0)^*(\mathbf{X},\mathbf{P},Q)\,\mathrm{d}\mathbf{X}, \tag{30}$$

the minimum being evaluated over a suitable set $\mathcal{K}$ of kinematically admissible deformation gradient fields with prescribed volume average $\overline{\mathbf{F}}$ as for (6). The further inequality

$$\overline{W}(\overline{\mathbf{F}},c) \geq \min_{\mathbf{F}\in\mathcal{K}} \int_\Omega f_0(\mathbf{X},\mathbf{F},J)\,\mathrm{d}\mathbf{X} + \min_{\mathbf{F}\in\mathcal{K}} \int_\Omega \mathbf{P}\cdot\mathbf{F}\,\mathrm{d}\mathbf{X} + \min_{\mathbf{F}\in\mathcal{K}} \int_\Omega Q\,J\,\mathrm{d}\mathbf{X} - \int_\Omega (f-f_0)^*(\mathbf{X},\mathbf{P},Q)\,\mathrm{d}\mathbf{X} \tag{31}$$

follows from a well-known property of the minimum of sums. The first term in (31) is nothing more than the effective stored-energy function of the comparison medium with local energy (27). We denote it by

$$\overline{W}_0(\overline{\mathbf{F}}) \doteq \min_{\mathbf{F}\in\mathcal{K}} \int_\Omega W_0(\mathbf{X},\mathbf{F})\,\mathrm{d}\mathbf{X}. \tag{32}$$

The second and third terms in (31) are bounded from below only so long as $\mathbf{P}$ is divergence-free and Q is a constant (and hence also divergence-free). For simplicity, we choose both these fields to be constant and denote them by $\mathbf{P}=\overline{\mathbf{P}}$ and $Q=\overline{Q}$. This gives

$$\overline{W}(\overline{\mathbf{F}},c) \geq \overline{W}_0(\overline{\mathbf{F}})+\overline{\mathbf{P}}\cdot\overline{\mathbf{F}}+\overline{Q}\,\overline{J}-\int_\Omega (f-f_0)^*(\mathbf{X},\overline{\mathbf{P}},\overline{Q})\,\mathrm{d}\mathbf{X}. \tag{33}$$

Relation (33) provides a lower bound for the effective stored-energy function $\overline{W}$ for the filled elastomer with local energy (26) in terms of the effective stored-energy function $\overline{W}_0$ for a comparison medium with local energy (27). It is valid for any choice of constants $\overline{\mathbf{P}}$ and $\overline{Q}$, and any choice of the function f_0 describing the local constitutive behavior and microstructure of the comparison medium. Optimization of (33) with respect to $\overline{\mathbf{P}}$ and $\overline{Q}$ leads to

$$\overline{W}(\overline{\mathbf{F}},c) \geq \overline{W}_0(\overline{\mathbf{F}})+\sup_{\overline{\mathbf{P}},\overline{Q}}\left[\overline{\mathbf{P}}\cdot\overline{\mathbf{F}}+\overline{Q}\,\overline{J}-\int_\Omega (f-f_0)^*(\mathbf{X},\overline{\mathbf{P}},\overline{Q})\,\mathrm{d}\mathbf{X}\right] = \overline{W}_0(\overline{\mathbf{F}})+\left(\int_\Omega (f-f_0)^*\,\mathrm{d}\mathbf{X}\right)^*(\overline{\mathbf{F}},\overline{J}). \tag{34}$$

Optimizing this result in turn with respect to f_0 leads formally to

$$\overline{W}(\overline{\mathbf{F}},c) \geq \sup_{f_0}\left\{\overline{W}_0(\overline{\mathbf{F}})+\left(\int_\Omega (f-f_0)^*\,\mathrm{d}\mathbf{X}\right)^*(\overline{\mathbf{F}},\overline{J})\right\}. \tag{35}$$

A partially optimized explicit formulation. The computation of the "optimal" bound (35) involves two technical difficulties. First, the polar function $(f-f_0)^*$ may have corners, and hence the computation of the Legendre transform of its average in (35) may require the use of subgradients as opposed to standard differentiation; see, e.g., Willis (1991) for similar difficulties in the classical context of convex energies. Second, the supremum operation in (35) involves optimization with respect to the local constitutive behavior of the comparison medium as well as with respect to its microstructure, which may require the computation of complicated integrals in the second term of (35). A detailed analysis of these two issues is a substantial task more appropriate for presentation elsewhere. In this work, we shall be content with employing a partially optimized version of the result (33) — and *not* the fully optimized bound (35) — which avoids the above-mentioned technical difficulties altogether.

A natural prescription to avoid the computation of subgradients in the above development is to set $\overline{\mathbf{P}}=\mathbf{0}$ and $\overline{Q}=0$. Then, after recognizing from (28) that

$$(f-f_0)^*(\mathbf{X},\mathbf{0},0) = \sup_{\mathbf{A},a}[-f(\mathbf{X},\mathbf{A},a)+f_0(\mathbf{X},\mathbf{A},a)] = -\min_{\mathbf{A},a}[f(\mathbf{X},\mathbf{A},a)-f_0(\mathbf{X},\mathbf{A},a)], \tag{36}$$

it follows from (33) that

$$\overline{W}(\overline{\mathbf{F}},c) \geq \overline{W}_0(\overline{\mathbf{F}})+\int_\Omega \min_{\mathbf{A},a}[f(\mathbf{X},\mathbf{A},a)-f_0(\mathbf{X},\mathbf{A},a)]\,\mathrm{d}\mathbf{X}. \tag{37}$$

[3] It is possible to invoke Legendre transformations that are more general and efficient than (28) (see, e.g., Chapter 6 in Dacorogna, 2008), but the choice (28) proves general enough for the isotropic material systems of interest in this work.

To avoid the computation of complicated integrals in the second term of (37), it is reasonable to restrict attention to a comparison medium in the form of a filled elastomer with the same microstructure as the actual filled elastomer, namely,

$$W_0(\mathbf{X},\mathbf{F}) = f_0(\mathbf{X},\mathbf{F},J) = (1-\theta(\mathbf{X}))f_{0_m}(\mathbf{F},J)+\theta(\mathbf{X})f_{0_p}(\mathbf{F},J), \tag{38}$$

where the indicator function θ is the same as in (26). Since the interest here is in elastomers reinforced by rigid particles, it suffices in fact to restrict attention to a comparison filled elastomer of the form (38) in which the particles are also rigid. Without loss of generality, this can be easily accomplished by setting

$$f_{0_p}(\mathbf{F},J) = f_p(\mathbf{F},J) = \frac{\mu_p}{2}[\mathbf{F}\cdot\mathbf{F}-3]+\mu_p\left[\frac{1}{2}(J-1)^2-(J-1)\right]. \tag{39}$$

Substituting (26) and (38) with (39) in (37) and then taking the limit of rigid particles $\mu_p\to+\infty$ renders,[4] with a slight change in notation,

$$\overline{W}(\overline{\mathbf{F}},c) \geq \overline{W}_0(\overline{\mathbf{F}},c)+(1-c)\min_{\mathbf{A},a}[f_m(\mathbf{A},a)-f_{0_m}(\mathbf{A},a)]. \tag{40}$$

This lower bound is non-trivial only so long as f_m grows faster than the choice of stored-energy function f_{0_m} for the comparison matrix material in the limit as $\|\mathbf{F}\|,|J|\to+\infty$. For the opposite case[5] when f_{0_m} grows faster than f_m as $\|\mathbf{F}\|,|J|\to+\infty$, the symmetry of (40) in the pairs $(\overline{W},f_m)$ and $(\overline{W}_0,f_{0_m})$ implies the following non-trivial upper bound

$$\overline{W}(\overline{\mathbf{F}},c) \leq \overline{W}_0(\overline{\mathbf{F}},c)+(1-c)\max_{\mathbf{A},a}[f_m(\mathbf{A},a)-f_{0_m}(\mathbf{A},a)]. \tag{41}$$

At this stage, it is a simple matter to combine the inequalities (40) and (41) to finally establish the main result of this section

$$\overline{W}(\overline{\mathbf{F}},c) = \begin{cases} \overline{W}_0(\overline{\mathbf{F}},c)+(1-c)\min\limits_{\mathbf{A},a}[f_m(\mathbf{A},a)-f_{0_m}(\mathbf{A},a)] & \text{if } f_m-f_{0_m}>-\infty \\ \overline{W}_0(\overline{\mathbf{F}},c)+(1-c)\max\limits_{\mathbf{A},a}[f_m(\mathbf{A},a)-f_{0_m}(\mathbf{A},a)] & \text{if } f_m-f_{0_m}<\infty, \end{cases} \tag{42}$$

where the equality has been used in the sense of a variational approximation. Expression (42) provides an explicit framework for constructing approximate solutions for the effective stored-energy function $\overline{W}$ of elastomers with (possibly compressible and anisotropic) stored-energy function $W(\mathbf{F})=f_m(\mathbf{F},J)$ reinforced by a finite concentration c of rigid particles directly in terms of the effective stored-energy function $\overline{W}_0$ of different elastomers with stored-energy function $W_0(\mathbf{F})=f_{0_m}(\mathbf{F},J)$ reinforced by exactly the same distribution of rigid particles (i.e., exactly the same indicator function θ). The framework is valid for any choice of the function f_{0_m}, which prompts the following optimization:

$$\overline{W}(\overline{\mathbf{F}},c) = \begin{cases} \sup\limits_{f_{0_m}}\{\overline{W}_0(\overline{\mathbf{F}},c)+(1-c)\min\limits_{\mathbf{A},a}[f_m(\mathbf{A},a)-f_{0_m}(\mathbf{A},a)]\} & \text{if } f_m-f_{0_m}>-\infty \\ \inf\limits_{f_{0_m}}\{\overline{W}_0(\overline{\mathbf{F}},c)+(1-c)\max\limits_{\mathbf{A},a}[f_m(\mathbf{A},a)-f_{0_m}(\mathbf{A},a)]\} & \text{if } f_m-f_{0_m}<\infty. \end{cases} \tag{43}$$

The usefulness of the formulation (43) — or more generally (42) — hinges upon having knowledge of the effective stored-energy function $\overline{W}_0$ for the comparison filled elastomer. While there have been no prior results available for such classes of materials (other than a few strictly in 2D), we now have at our disposal the results for filled Neo-Hookean rubber worked out in the preceding section.

4.2. Application to filled non-Gaussian rubber

Below, we make use of the filled Neo-Hookean rubber considered in Section 3 as the choice for the comparison medium in the formulation (43) in order to construct an approximate solution for the effective stored-energy function (10) for filled non-Gaussian rubber. To this end, we set

$$f_m(\mathbf{F},J) = \Psi(I_1)+\frac{\mu+\mu'}{2}(J-1)^2-\mu(J-1) \quad \text{and} \quad f_{0_m}(\mathbf{F},J) = \frac{\mu_0}{2}[I_1-3]+\frac{\mu_0+\mu'}{2}(J-1)^2-\mu_0(J-1), \tag{44}$$

where μ' and μ_0 are positive material parameters, and note that in the limit as $\mu'\to+\infty$ these regularized compressible energies reduce identically to the incompressible non-Gaussian and Neo-Hookean stored-energy functions

$$f_m(\mathbf{F},J) = \begin{cases} \Psi(I_1) & \text{if } J=1 \\ +\infty & \text{otherwise} \end{cases} \quad \text{and} \quad f_{0_m}(\mathbf{F},J) = \begin{cases} \frac{\mu_0}{2}[I_1-3] & \text{if } J=1 \\ +\infty & \text{otherwise} \end{cases} \tag{45}$$

of interest here.

[4] An alternative direct derivation of the formula (40) follows *mutatis mutandis* from a derivation of Willis (see, e.g., Eq. (3.3) in Willis, 1991; Eq. (8.17) in Willis, 2002; see also deBotton and Shmuel, 2010) of Ponte Castañeda's (1991) bound in the context of convex energies: $\overline{W}=\min_{\mathbf{F}\in\mathcal{K}}\int_\Omega[W_0+(W-W_0)]\,d\mathbf{X}\geq\overline{W}_0+\int_\Omega\min(W-W_0)\,d\mathbf{X}$.

[5] For the isotropic matrix materials of interest in this work, mixed cases in which f_{0_m} grows faster (slower) in $\mathbf{F}$ but slower (faster) in J than f_m need not be considered.

Upon substitution of (44) in the general formulation (43), it is straightforward to show that

$$\overline{W}(\overline{\mathbf{F}},c)=\begin{cases}\begin{cases}\max\limits_{\mu_0}\left\{\overline{W}_0(\overline{\mathbf{F}},c)+(1-c)\min\limits_{\mathcal{I}_1}\left[\Psi(\mathcal{I}_1)-\dfrac{\mu_0}{2}[\mathcal{I}_1-3]\right]\right\} & \text{if } \Psi(\mathcal{I}_1)-\mathcal{I}_1>-\infty\\ \min\limits_{\mu_0}\left\{\overline{W}_0(\overline{\mathbf{F}},c)+(1-c)\max\limits_{\mathcal{I}_1}\left[\Psi(\mathcal{I}_1)-\dfrac{\mu_0}{2}[\mathcal{I}_1-3]\right]\right\} & \text{if } \Psi(\mathcal{I}_1)-\mathcal{I}_1<\infty\end{cases} & \text{if } \bar{J}=1\\ +\infty & \text{otherwise}\end{cases} \tag{46}$$

in the limit as $\mu'\to+\infty$, where the macroscopic incompressibility constraint $\bar{J}=1$ in (46) ensuing from the microscopic incompressibility constraint $J=1$ in (45) and the rigid behavior (3) of the particles is the expected exact constraint. The result (46) is applicable to any distribution of rigid particles (i.e., any indicator function θ). By restricting attention to the isotropic distributions of rigid particles of polydisperse sizes of interest here and invoking the notation introduced in (10) together with the result (23) for filled Neo-Hookean rubber, the finite branch of the energy (46) specializes to

$$\overline{\Psi}(\bar{I}_1,\bar{I}_2,c)=\begin{cases}\max\limits_{\mu_0}\left\{\dfrac{\mu_0}{2(1-c)^{5/2}}[\bar{I}_1-3]+(1-c)\min\limits_{\mathcal{I}_1}\left[\Psi(\mathcal{I}_1)-\dfrac{\mu_0}{2}[\mathcal{I}_1-3]\right]\right\} & \text{if } \Psi(\mathcal{I}_1)-\mathcal{I}_1>-\infty\\ \min\limits_{\mu_0}\left\{\dfrac{\mu_0}{2(1-c)^{5/2}}[\bar{I}_1-3]+(1-c)\max\limits_{\mathcal{I}_1}\left[\Psi(\mathcal{I}_1)-\dfrac{\mu_0}{2}[\mathcal{I}_1-3]\right]\right\} & \text{if } \Psi(\mathcal{I}_1)-\mathcal{I}_1<\infty\end{cases}. \tag{47}$$

In view of the property $(9)_1$ of the function Ψ, it is not difficult to deduce that the max–min and the min–max problems in (47) are solved by exactly the same stationarity conditions[6]

$$\frac{\partial\Psi}{\partial\mathcal{I}_1}(\mathcal{I}_1)=\frac{\mu_0}{2}\quad\text{and}\quad\mathcal{I}_1=\frac{\bar{I}_1-3}{(1-c)^{7/2}}+3 \tag{48}$$

irrespectively of the growth conditions of Ψ, and hence that the energy (47) can be compactly written as

$$\overline{\Psi}(\bar{I}_1,\bar{I}_2,c)=(1-c)\Psi\left(\frac{\bar{I}_1-3}{(1-c)^{7/2}}+3\right). \tag{49}$$

The simple explicit effective stored-energy function (49) constitutes the main result of this paper. It characterizes the overall nonlinear elastic response of non-Gaussian rubber with stored-energy function $\Psi(I_1)$ filled with an isotropic distribution of rigid particles of polydisperse sizes and finite concentration c. The following theoretical and practical remarks are in order:

(i) Owing to the properties (8) and $(9)_1$ of the function Ψ, the effective stored-energy function (49) is such that

$$\begin{aligned}&\overline{\Psi}(3,3,c)=0,\\ &\overline{\Psi}(\bar{I}_1,\bar{I}_2,c)>0\quad\forall\bar{I}_1,\bar{I}_2>3,\\ &\overline{\Psi}(\bar{I}_1,\bar{I}_2,c_2)>\overline{\Psi}(\bar{I}_1,\bar{I}_2,c_1)\quad\forall\bar{I}_1,\bar{I}_2>3,c_2>c_1\geq0.\end{aligned} \tag{50}$$

The first two of these conditions are direct consequences of the fact that the filled non-Gaussian rubber is stress-free in the undeformed configuration, isotropic, and incompressible. The last condition entails physically that the addition of rigid particles consistently leads to a stiffer material response irrespectively of the applied loading, in agreement with experience.

(ii) Remarkably, the effective stored-energy function (49) is independent of the second principal invariant $\bar{I}_2=\overline{\mathbf{F}}^{-T}\cdot\overline{\mathbf{F}}^{-T}$. The origin of this independence can be traced back to the first step of the derivation, when the weak but existent dependence on $\bar{I}_2$ of the dilute response of filled Neo-Hookean rubber (see Sections 3.2 and 5 in Part I) was neglected in order to favor analytical tractability. Neither the iterated dilute homogenization procedure to account for finite concentration of particles (Section 3.1), nor the comparison medium procedure to account for non-Gaussian behavior (Section 4.1) introduced dependence on $\bar{I}_2$ thereafter. This suggests — given the different nature and generality of these two procedures — that the response of any filled I_1-based non-Gaussian elastomer is in all likelihood practically insensitive to $\bar{I}_2$. The FE simulations presented in the next section provide further support that this is indeed the case.

(iii) For the common case when the stored-energy function Ψ for the underlying non-Gaussian matrix material is convex in I_1,

$$\frac{\mathrm{d}\Psi}{\mathrm{d}I_1}(I_1)>0\quad\text{and}\quad\frac{\mathrm{d}^2\Psi}{\mathrm{d}I_1^2}(I_1)\geq0, \tag{51}$$

it is a simple matter to deduce that

$$\frac{\partial\overline{\Psi}}{\partial\bar{I}_1}(\bar{I}_1,\bar{I}_2,c)>0,$$

[6] It is of practical relevance to note here that the optimal values of the variables μ_0 and $\mathcal{I}_1$ dictated by (48) are physically consistent in the sense that $\mu_0\geq0$ and $\mathcal{I}_1\geq3$.

$$\frac{\partial \overline{\Psi}}{\partial \bar{I}_1}(\bar{I}_1,\bar{I}_2,c)+2[\bar{I}_1-\overline{\lambda}_k^{-2}-2\overline{\lambda}_k^{-1}]\frac{\partial^2 \overline{\Psi}}{\partial \bar{I}_1^2}(\bar{I}_1,\bar{I}_2,c)>0 \quad (k=1,2,3), \quad \forall \bar{I}_1,\bar{I}_2\geq 3, c\geq 0, \tag{52}$$

and hence that the effective stored-energy function (49) is strongly elliptic (see, e.g., Section 4 in Zee and Sternberg, 1983). This stability property is consistent with recent 2D bifurcation analyses (Triantafyllidis et al., 2007; Michel et al., 2010) which have shown that isotropic filled elastomers that are microscopically (i.e., pointwise) convex in I_1 are macroscopically strongly elliptic. For the case when Ψ is merely strongly elliptic (i.e., it satisfies the weaker conditions (9)) but not convex in I_1, the effective stored-energy function (49) can still be shown to be strongly elliptic for small enough deformations, but it may lose strong ellipticity at sufficiently large values of $\bar{I}_1>3$.

(iv) In the limit of small deformations ($\bar{I}_1,\bar{I}_2\to 3$), the stored-energy function (49) reduces asymptotically to

$$\overline{\Psi}(\bar{I}_1,\bar{I}_2,c)=\overline{\mu}\,[\overline{\varepsilon}_1^2+\overline{\varepsilon}_2^2+\overline{\varepsilon}_3^2] \quad \text{with} \quad \overline{\varepsilon}_1+\overline{\varepsilon}_2+\overline{\varepsilon}_3=0 \tag{53}$$

to leading order in the deformation measures $\overline{\varepsilon}_k=\overline{\lambda}_k-1$ ($k=1,2,3$), where it is recalled that $\overline{\lambda}_k$ denote the singular values of the macroscopic deformation gradient $\overline{\mathbf{F}}$ and

$$\overline{\mu}=\frac{\mu}{(1-c)^{5/2}} \tag{54}$$

stands for the initial effective shear modulus of the filled rubber. Expression (54) agrees identically with the exact Brinkman–Roscoe result (cf. Eq. (12) in Roscoe, 1973) for the effective shear modulus of an isotropic incompressible linearly elastic solid reinforced by an isotropic distribution of rigid spherical particles of infinitely many diverse sizes. In the further limit of small concentration of particles as $c\to 0$, the effective shear modulus (54) reduces to

$$\overline{\mu}=\mu+\frac{5}{2}\mu\, c+O(c^2), \tag{55}$$

which agrees in turn with the classical Einstein-Smallwood result (cf. Eq. (12) in Smallwood, 1944) for the effective shear modulus of an isotropic incompressible linearly elastic solid reinforced by a dilute distribution of rigid spherical particles.

(v) The connection with the effective shear modulus (54) for isotropic distributions of spherical particles is not restricted to small deformations. Indeed, for the special case when the elastomeric matrix is Neo-Hookean rubber, $\Psi=\mu/2[I_1-3]$ and the effective stored-energy function (49) reduces to

$$\overline{\Psi}(\bar{I}_1,\bar{I}_2,c)=\frac{\mu}{2(1-c)^{5/2}}[\bar{I}_1-3], \tag{56}$$

which is seen to have the same functional form as the Neo-Hookean matrix material, with the effective shear modulus given by (54). While the effective stored-energy function (56) is not an exact realizable result for Neo-Hookean rubber filled with an isotropic distribution of rigid spherical particles of polydisperse sizes, owing to its iterative construction process (see Section 3.1), it is expected to provide a very accurate approximation for this class of material systems. By the same token, the approximate effective stored-energy function (49) is expected to describe very accurately the response of any non-Gaussian rubber filled with an isotropic distribution of rigid spherical particles of polydisperse sizes in the small and moderate deformation regimes. For large deformations, the result (49) is likely to be relatively less accurate for this class of material systems, as its variational construction process (see Section 4.1) entails that it corresponds to some sort of lower (upper) bound when the underlying matrix material has stronger (weaker) growth conditions than Neo-Hookean rubber. These expectations are supported by comparisons with the FE simulations presented in the next section.

(vi) Rather interestingly, the result (49) indicates that the nonlinear elastic response of filled non-Gaussian rubber corresponds in essence to the response of the underlying non-Gaussian rubber — as characterized by its stored-energy function Ψ — evaluated at the "amplified" measure of strain

$$\bar{I}_1^{Amp}=\frac{\bar{I}_1-3}{(1-c)^{7/2}}+3. \tag{57}$$

The idea of modeling the behavior of filled elastomers as the behavior of the underlying matrix material evaluated at some amplified measure of strain was originally proposed by Mullins and Tobin (1965) on heuristic grounds. The homogenization result (49) derived in this work suggests that this empirical idea is roughly correct, at least for filled I_1-based non-Gaussian rubber, and that the strain measure that is amplified is the first principal invariant I_1.

5. FE simulations of suspensions of rigid spherical particles in rubber under large deformations

In order to compare the above theoretical results with a separate solution, in this section we work out full 3D finite-element (FE) simulations of the large-deformation response of Neo-Hookean and non-Gaussian rubber reinforced by random isotropic distributions of rigid spherical particles. To simulate the randomness and isotropy of the microstructure, we consider infinite periodic media made up of the repetition of cubic unit cells of unit volume $L^3=1$ containing a random distribution of a large number of particles. With the aim of gaining insight into the effect of the size dispersion of the filler particles, we examine distributions with particles of the same (monodisperse) and of different (polydisperse) sizes.

5.1. Monodisperse microstructures

The monodisperse microstructures are constructed by means of a random sequential adsorption algorithm (see, e.g., Chapter 3 in Torquato, 2002 and references therein) in which the sequential addition of particles is constrained so that the distance between the particles with other particles and with the boundaries of the cubic unit cell take a minimum value that guaranties adequate spatial discretization (see, e.g., Segurado and Llorca, 2002; Fritzen et al., 2012), namely:

- The center-to-center distance between a new particle i in the sequential algorithm and any previously accepted particle $j=1,2,\ldots,i-1$ has to exceed the minimum value $s_1=2R_m(1+d_1)$, where the offset distance d_1 is fixed here at $d_1=0.02$. This condition can be compactly written in the form
$$\|\mathbf{X}^i-\mathbf{X}^j-\mathbf{h}\|\geq s_1, \tag{58}$$
where $\mathbf{X}^i$ ($\mathbf{X}^j$) denotes the location of the center of particle i (j) and $\mathbf{h}$ is a vector with entries 0, L, or $-L$ for each of its three Cartesian components with respect to the principal axes of the cubic unit cell.[7]
- The particles should be sufficiently distant from the boundaries of the unit cell as enforced by the inequalities
$$|X^i_k-R_m|\geq s_2 \quad \text{and} \quad |X^i_k+R_m-L|\geq s_2 \quad (k=1,2,3), \tag{59}$$
where $s_2=d_2R_m$ with d_2 being fixed here at $d_2=0.05$.

In the above expressions,
$$R_m=L\left(\frac{3c}{4\pi N}\right)^{1/3} \tag{60}$$
stands for the radius of the particles, where N has been introduced to denote the number of particles in the unit cell. For the material systems of interest in this work, a parametric study varying the number of particles in the range $N\in[5,35]$ indicates that $N=30$ is a sufficiently large number to approximate overall isotropy; more specific comments on the degree of isotropy resulting by the use of $N=30$ are deferred to Section 5.4. Fig. 1 shows representative unit cells generated by the above-described algorithm for $N=30$ with three different particle concentrations: (a) $c=0.05$, (b) $c=0.15$, and (c) $c=0.25$.

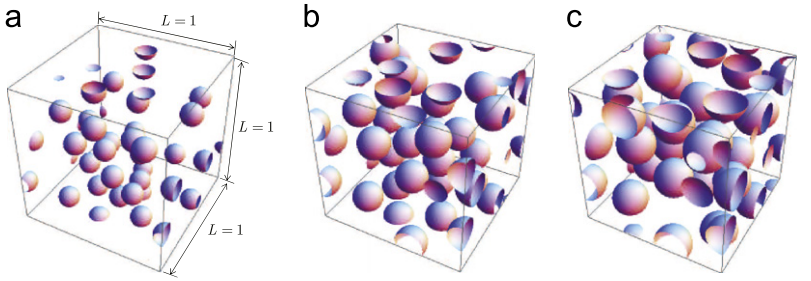

Fig. 1. Representative unit cells of unit volume $L^3=1$ containing $N=30$ randomly distributed spherical particles of monodisperse sizes with three different concentrations: (a) $c=0.05$, (b) $c=0.15$ and (c) $c=0.25$.

5.2. Polydisperse microstructures

The polydisperse microstructures are constructed by means of a similar constrained adsorption algorithm. The focus is on polydisperse microstructures with three different families of particle sizes. While there is no distinct rule for the creation of such microstructures and the possibilities are many, we consider for definiteness the following procedure:

- Three different families of particles with radii $R_p^{(I)}$ and concentrations $c^{(I)}$ ($I=1,2,3$) are utilized such that
$$\{R_p^{(1)},R_p^{(2)},R_p^{(3)}\}=\left\{R_p,\frac{7}{9}R_p,\frac{4}{9}R_p\right\} \quad \text{with} \quad R_p=L\left(\frac{3c^{(1)}}{4\pi N_p}\right)^{1/3}, \tag{61}$$
and
$$\{c^{(1)},c^{(2)},c^{(3)}\}=\{0.5c,0.25c,0.25c\} \quad \text{with} \quad c^{(1)}+c^{(2)}+c^{(3)}=c, \tag{62}$$
where N_p stands for the number of particles with the largest radius $R_p^{(1)}=R_p$ in the unit cell.
- The microstructures are generated sequentially by first adding particles with the largest radius $R_p^{(1)}$ until the concentration reaches the value $c^{(1)}=0.5c$, subsequently adding particles with radius $R_p^{(2)}$ until $c^{(1)}+c^{(2)}\simeq 0.75c$, and

[7] Note that condition (58) accounts for the fact that the excess of particles exceeding the spatial domain of the unit cell are appropriately relocated within the unit cell as dictated by the periodicity of the microstructure (see Fig. 1).

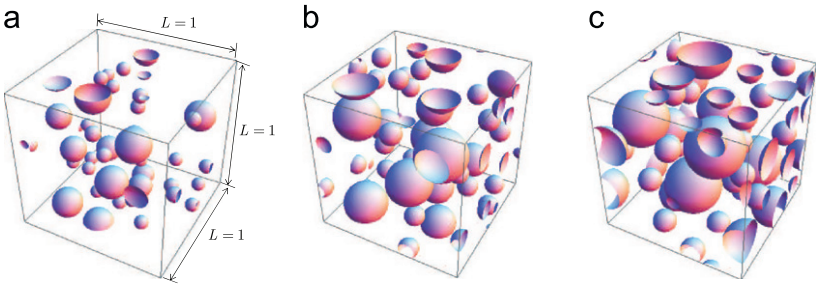

Fig. 2. Representative unit cells of unit volume $L^3=1$ containing $N=36$ randomly distributed spherical particles of three different sizes with three different concentrations: (a) $c\simeq 0.05$, (b) $c\simeq 0.15$ and (c) $c\simeq 0.25$.

finally adding particles with the smallest radius $R_p^{(3)}$ until $c^{(1)}+c^{(2)}+c^{(3)}\simeq c$. In following this construction process, we note that a target concentration c can only be achieved approximately (up to a small error that depends on the various choices of the parameters). To guarantee adequate spatial discretization, similar to conditions (58)–(59), the randomly generated placements of the centers of the particles are enforced to satisfy the following constraints:

$$\|\mathbf{X}^i-\mathbf{X}^j-\mathbf{h}\|\geq s_1,\quad s_1=(R_p^{(m_i)}+R_p^{(m_j)})(1+d_1), \tag{63}$$

$$\left|X_k^i-R_p^{(m_i)}\right|\geq s_2,\quad \left|X_k^i+R_p^{(m_i)}-1\right|\geq s_2,\quad s_2=d_2R_p^{(m_i)}\quad (k=1,2,3), \tag{64}$$

for $i,j=1,2,\ldots,N$ with N again denoting the total number of particles in the unit cell. Here, the offset parameters are set at $d_1=0.02$ and $d_2=0.05$ as in the monodisperse case, and the superscript $m_i=1,2,3$ has been introduced to denote the size of the sphere that should be added at step i in the sequential construction process, namely, $m_i=1$ if $c^{(m_i)}\leq c^{(1)}$, $m_i=2$ if $c^{(1)}<c^{(m_i)}\leq c^{(1)}+c^{(2)}$, and $m_i=3$ if $c^{(1)}+c^{(2)}<c^{(m_i)}$.

Guided by a parametric study, in this work we utilize $N_p=10$ which results into unit cells containing a total of $N=36$ particles. As discussed in Section 5.4, such unit cells are sufficiently large to be representative of isotropic microstructures. Fig. 2 displays sample unit cells generated by the above-described algorithm for $N=36$ with three different particle concentrations: (a) $c\simeq 0.05$, (b) $c\simeq 0.15$ and (c) $c\simeq 0.25$.

5.3. Meshing, material properties, and computation of the overall nonlinear elastic response

Having identified the monodisperse and polydisperse microstructures of interest, we now turn to their discretization. We make use of the mesh generator code Netgen (Schöberl, 1997), which has the capability to create periodic meshes as required here. Ten-node tetrahedral hybrid elements are utilized in order to handle exactly (in a numerical sense) the incompressible behavior of the elastomeric matrix and of the rigid particles. Since the computations are carried out using the FE package ABAQUS, we make use in particular of the C3D10H hybrid elements available in this code (see ABAQUS Version 6.11 Documentation, 2011). Fig. 3 shows three meshes of increasing refinement for a distribution of monodisperse particles with concentration $c=0.25$. Mesh sensitivity studies reveal that meshes with approximately 75,000 elements (such as the fine mesh shown in Fig. 3(b)) produce sufficiently accurate results.

Within the present formulation, the behavior of the matrix phase can be modeled exactly by any incompressible stored-energy function (7) of choice. On the other hand, the perfectly rigid behavior (3) of the particles can only be modeled approximately by means of a very (but not infinitely) stiff material. Here, for definiteness, we model the particles as incompressible Neo-Hookean solids with stored-energy function

$$W_p^{FE}(\mathbf{F})=\begin{cases}\dfrac{\mu_p^{FE}}{2}[I_1-3] & \text{if } J=1,\\ +\infty & \text{otherwise,}\end{cases} \tag{65}$$

where the parameter μ_p^{FE} is set to be three orders of magnitude larger than the initial shear modulus of the underlying matrix material, i.e., $\mu_p^{FE}=10^3\times\mu$.

By virtue of their periodicity, the overall nonlinear elastic response of any of the above-defined classes of filled elastomers amounts to subjecting their defining cubic unit cells to the periodic boundary conditions

$$\begin{aligned}&u_k(L,X_2,X_3)-u_k(0,X_2,X_3)=(\overline{F}_{k1}-\delta_{k1})L,\\ &u_k(X_1,L,X_3)-u_k(X_1,0,X_3)=(\overline{F}_{k2}-\delta_{k2})L,\\ &u_k(X_1,X_2,L)-u_k(X_1,X_2,0)=(\overline{F}_{k3}-\delta_{k3})L\end{aligned} \tag{66}$$

$(k=1,2,3)$, and computing the resulting total elastic energy $\overline{W}$, from which the macroscopic first Piola–Kirchhoff stress $\overline{\mathbf{S}}$ can then be determined; alternatively, $\overline{\mathbf{S}}$ can be computed directly by averaging the resulting local stresses $\mathbf{S}(\mathbf{X})$ over the

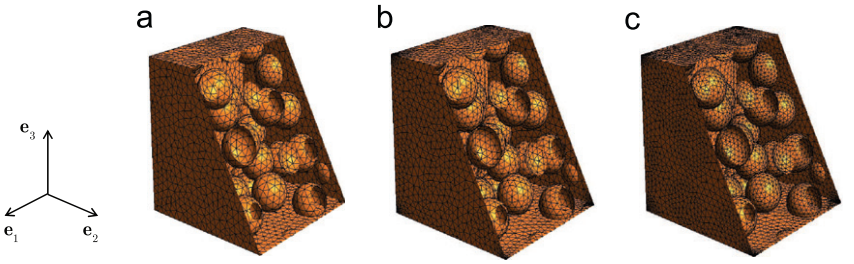

Fig. 3. Three representative meshes in the undeformed configuration for a distribution of monodisperse particles with concentration $c=0.25$: (a) coarse mesh with 34,629 elements, (b) fine mesh with 69,556 elements, and (c) very fine mesh with 170,203 elements.

undeformed unit cell. In expression (66), the components u_k and X_k ($k=1,2,3$) refer to a Cartesian frame of reference with origin placed at a corner of the cubic unit cell whose axes $\{\mathbf{e}_k\}$ are aligned with the principal axes of the cubic unit cell (see Fig. 3), δ_{kl} denotes the Kronecker delta, and $\overline{\mathbf{F}}$ is the prescribed average deformation gradient. As a practical remark, we note that the periodic boundary conditions (66) can be expediently implemented in ABAQUS by using the "Equation" option to couple the nodes of opposite sides of the cubic unit cells.

5.4. Assessment of the simulated microstructures

Because of the finite number of particles — $N=30$ for the monodisperse and $N=36$ for the polydisperse microstructures — included per unit cell, the microstructures simulated here are (not exactly but) only approximately isotropic. In order to assess their isotropy, we have constructed and compared three different realizations for each concentration of particles that is simulated. For all matrix materials, loading conditions, and particle concentrations considered, the maximum difference in the total elastic energy between any two corresponding realizations has been computed to be less than 0.5%.

Further, for each realization, we have examined the co-axiallity between the average Cauchy stress tensor $\overline{\mathbf{T}}\doteq\overline{\mathbf{S}}\overline{\mathbf{F}}^T$ and the average left Green-Cauchy strain tensor $\overline{\mathbf{B}}\doteq\overline{\mathbf{F}}\overline{\mathbf{F}}^T$ under three types of loading conditions: (i) axisymmetric tension where $\overline{\mathbf{F}}=\overline{\lambda}\mathbf{e}_1\otimes\mathbf{e}_1+\overline{\lambda}^{-1/2}(\mathbf{e}_2\otimes\mathbf{e}_2+\mathbf{e}_3\otimes\mathbf{e}_3)$ with $\overline{\lambda}\geq 1$, (ii) axisymmetric compression where $\overline{\mathbf{F}}=\overline{\lambda}\mathbf{e}_1\otimes\mathbf{e}_1+\overline{\lambda}^{-1/2}(\mathbf{e}_2\otimes\mathbf{e}_2+\mathbf{e}_3\otimes\mathbf{e}_3)$ with $\overline{\lambda}\leq 1$, and (iii) simple shear where $\overline{\mathbf{F}}=\mathbf{I}+\overline{\gamma}\mathbf{e}_1\otimes\mathbf{e}_2$ with $\overline{\gamma}\geq 0$. For all matrix materials, loading conditions, and particle concentrations considered, the maximum difference between any two corresponding principal axes of $\overline{\mathbf{T}}$ and $\overline{\mathbf{B}}$ has been computed to be less than 0.05 radians.

The above two sets of checks indicate that the monodisperse (polydisperse) microstructures with $N=30$ ($N=36$) particles per unit cell utilized in this work are indeed good approximations of isotropic distributions of spherical particles.

In the comparisons with the analytical solution (49) that follow in the next section, all presented FE results correspond to the average of three realizations. Moreover, all FE results are computed by following an incremental loading path, at each step of which the incremental equilibrium equations are solved directly in ABAQUS. We utilize the default dual convergence criterion in this code (see ABAQUS Version 6.11 Documentation, 2011), namely, the permissible ratio of the largest solution correction to the largest corresponding incremental solution is set at $|\Delta\mathbf{u}|/|\mathbf{u}_{max}|=10^{-2}$, while the permissible ratio of the largest residual to the corresponding average force norm is set at $R_{tol}=5\times 10^{-3}$. Whenever one of these criteria is not satisfied the computations are stopped. This typically happens whenever the elements in between two particles become exceedingly distorted because of the locally large deformations involved.

Fig. 4 presents an example of large local deformations in between particles for the case of a monodisperse realization with $c=0.25$ and Neo-Hookean matrix under simple shear. Part (a) shows contour plots of the maximum principal

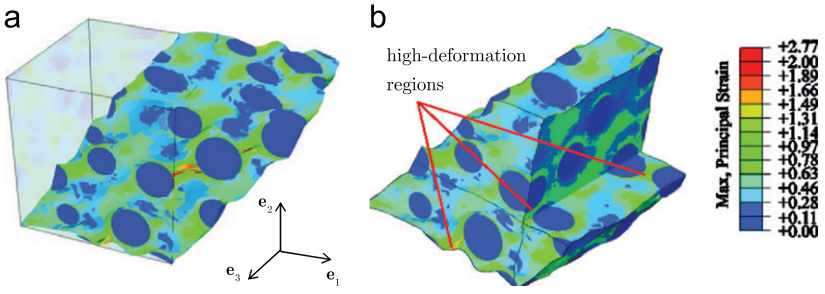

Fig. 4. (a) Contour plots of the maximum principal logarithmic strain for a monodisperse realization with $c=0.25$ and Neo-Hookean matrix subjected to an overall simple shear strain of $\overline{\gamma}=0.64$; the undeformed configuration is also depicted for comparison purposes. Part (b) shows an inside view of three pairs of particles in between which the matrix material is highly deformed.

logarithmic strain at an overall shear strain level of $\overline{\gamma}=0.64$; the initial undeformed geometry is also depicted for comparison purposes. The deformation contours are seen to be highly heterogeneous with principal logarithmic strains as large as 2.77 within regions between particles. In part (b), an inside view is shown of three regions of strong particle interaction and high local strains that lead to significant mesh distortion and therefore problems with the numerical convergence of the FE calculations. In principle, re-meshing of these regions should allow to reach further overall deformations (see, e.g., Moraleda et al., 2009 for the analogous problem in 2D), but this is beyond the scope of this work and hence not pursued here.

6. Sample results and discussion

A range of specific results are presented next for the overall nonlinear elastic response of filled rubber as described by the analytical approximation (49) and the FE simulations of Section 5. Results for the linear elastic response in the small-deformation regime are presented first followed by results for the large-deformation response of filled Neo-Hookean rubber under various loading conditions. The third set of results pertains to the response of a filled rubber wherein the underlying elastomeric matrix is characterized by the non-Gaussian stored-energy function (Lopez-Pamies, 2010b)

$$\Psi(I_1)=\frac{3^{1-\alpha_1}}{2\alpha_1}\mu_1[I_1^{\alpha_1}-3^{\alpha_1}]+\frac{3^{1-\alpha_2}}{2\alpha_2}\mu_2[I_1^{\alpha_2}-3^{\alpha_2}] \tag{67}$$

with $\mu_1=0.032$ MPa, $\mu_2=0.3$ MPa, $\alpha_1=3.837$, $\alpha_2=0.559$, corresponding to a model that has been shown to accurately describe the nonlinear elastic response of typical silicone rubber over large ranges of deformations (see Section 2.3 in Lopez-Pamies, 2010b).

The selection of results presented here aims at providing further insight into the constructed analytical solution (49) and at assessing its accuracy for a wide range of particle concentrations, elastomeric matrix materials, and loading conditions. The results also aim at shedding light on the effect of the size dispersion of fillers in the overall nonlinear elastic response of filled elastomers.

6.1. Linear elastic results

In the limit of small deformations (see remark (iv) in Section 4.2), the analytical approximation (49) reduces to the exact effective stored-energy function (53) with (54) for an isotropic incompressible linearly elastic solid reinforced by an isotropic distribution of rigid spherical particles of infinitely many diverse sizes. Fig. 5 presents plots for the initial effective shear modulus (54), normalized by the initial shear modulus μ of the underlying elastomeric matrix, as a function of the concentration of particles c. Results are also presented for the FE simulations of Section 5 for isotropic distributions of spherical particles with the same size (monodisperse) and with three different sizes (polydisperse). To gain further insight, the corresponding Hashin–Shtrikman lower bound for the effective shear modulus of rigidly reinforced, isotropic, incompressible, linearly elastic materials (Hashin and Shtrikman, 1961) is included in the figure. As expected, all four results stiffen monotonically with increasing values of c. Although exact for infinitely polydisperse particles, the analytical response is seen to be in good agreement with the FE results

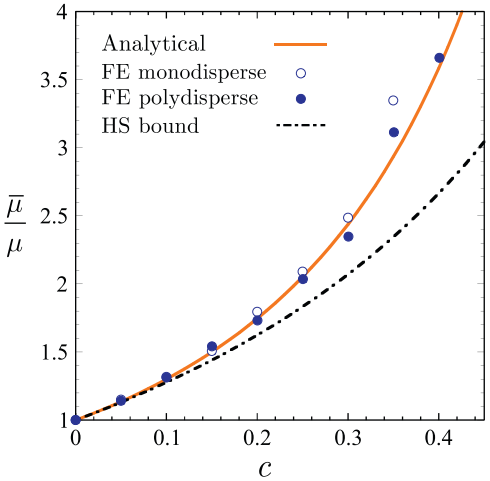

Fig. 5. The normalized initial effective shear modulus $\overline{\mu}/\mu$ of isotropic incompressible elastomers filled with random isotropic distributions of rigid particles. Plots are shown for: (i) the analytical result (54), (ii) FE simulations for distributions of spherical particles with the same (monodisperse) and with three different (polydisperse) sizes, and (iii) the corresponding Hashin–Shtrikman lower bound $\overline{\mu}/\mu=(2+3c)/(2-2c)$, as functions of the concentration of particles c.

for polydisperse particles with only three families of particle sizes for the entire range of concentrations considered $c \in [0,0.4]$. More remarkably, the analytical solution exhibits good agreement with the FE results for monodisperse particles up to the relatively high concentration of $c=0.3$. These favorable comparisons are consistent with earlier 2D results (Moraleda et al., 2009; Lopez-Pamies, 2010a) suggesting that polydispersity does *not* play a role in the response of particle-reinforced materials for particle concentrations sufficiently below the percolation limit. A further relevant observation from Fig. 5 is that all three particulate results (analytical, FE monodisperse, FE polydisperse) are very close to the Hashin–Shtrikman lower bound up to a concentration of particles of about $c=0.1$, after which they become significantly stiffer.

6.2. Results for filled Neo-Hookean rubber

For the case when the underlying matrix material is Neo-Hookean rubber (see remark v in Section 4.2), the analytical approximation (49) takes the form (56). Fig. 6 presents results for the large-deformation response of filled Neo-Hookean rubber, as characterized by the effective stored-energy function (56), for three values of particle concentration $c=0.05$, 0.15, and 0.25 under: (a) uniaxial compression, (b) uniaxial tension, (c) pure shear, and (d) simple shear. The constitutive stress-deformation relations for these loading conditions read explicitly as

- *Uniaxial loading* ($\overline{\lambda}_1=\overline{\lambda}$, $\overline{\lambda}_2=\overline{\lambda}_3=\overline{\lambda}^{-1/2}$ with $\overline{t}_2=\overline{t}_3=0$):

$$\overline{S}_{un}=\overline{\lambda}^{-1}\overline{t}_1=\frac{d\overline{\Psi}}{d\overline{\lambda}}=\frac{\mu}{(1-c)^{5/2}}[\overline{\lambda}-\overline{\lambda}^{-2}] \tag{68}$$

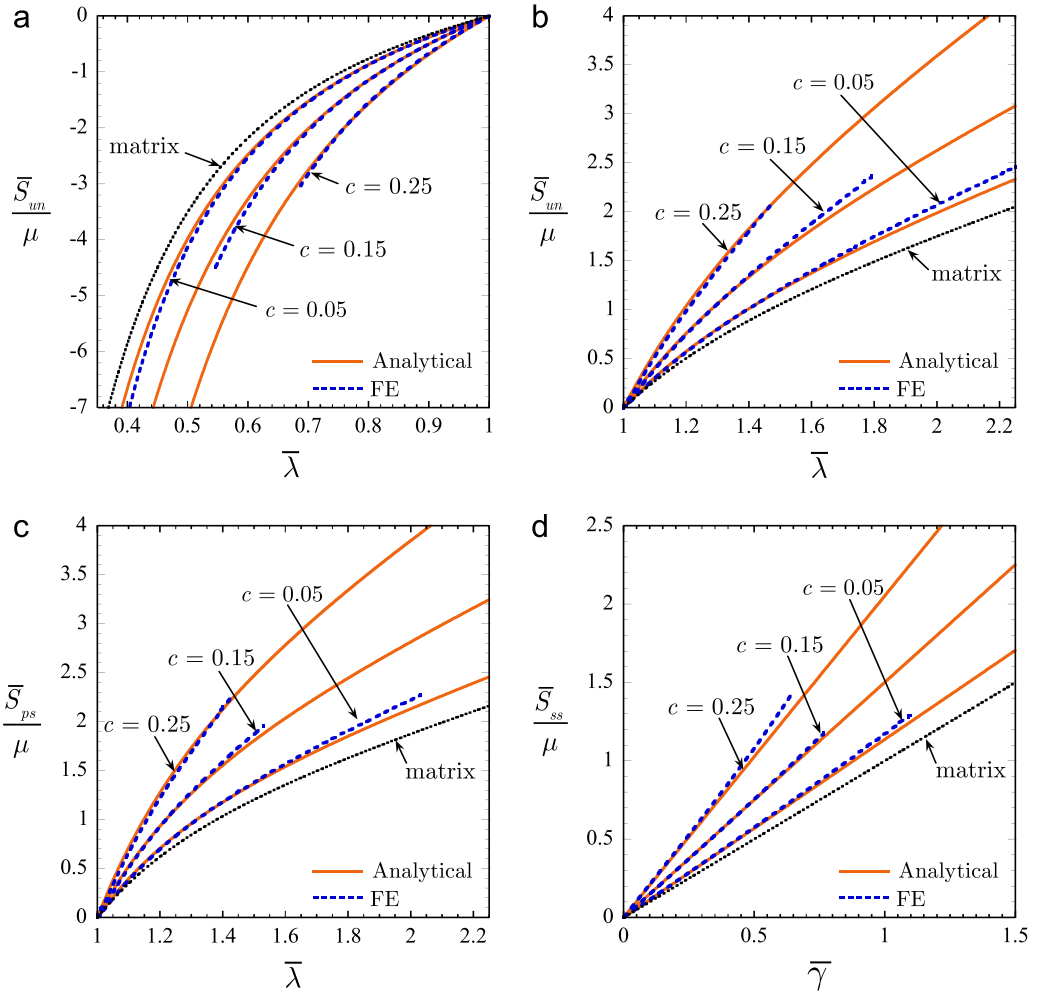

Fig. 6. Macroscopic response of filled Neo-Hookean rubber with various values of concentration of particles c under: (a) uniaxial compressive, (b) uniaxial tensile, (c) pure shear, and (d) simple shear loading conditions. Plots are shown for the analytical stress-deformation results (68)–(70), and corresponding FE simulations for isotropic distributions of spherical particles.

- *Pure shear* ($\overline{\lambda}_1=\overline{\lambda}$, $\overline{\lambda}_2=\overline{\lambda}^{-1}$, $\overline{\lambda}_3=1$ with $\overline{t}_2=0$):

$$\overline{S}_{ps}=\overline{\lambda}^{-1}\overline{t}_1=\frac{\mathrm{d}\overline{\Psi}}{\mathrm{d}\overline{\lambda}}=\frac{\mu}{(1-c)^{5/2}}[\overline{\lambda}-\overline{\lambda}^{-3}] \tag{69}$$

- *Simple shear* ($\overline{\lambda}_1=(\overline{\gamma}+\sqrt{\overline{\gamma}^2+4})/2$, $\overline{\lambda}_2=\overline{\lambda}_1^{-1}$, $\overline{\lambda}_3=1$):

$$\overline{S}_{ss}=\frac{\mathrm{d}\overline{\Psi}}{\mathrm{d}\overline{\gamma}}=\frac{\mu}{(1-c)^{5/2}}\,\overline{\gamma}, \tag{70}$$

where $\overline{S}_{un}$, $\overline{S}_{ps}$, $\overline{S}_{ss}$ denote first Piola–Kirchhoff stress measures, while $\overline{t}_1$, $\overline{t}_2$, $\overline{t}_3$ have been introduced to denote the macroscopic principal Cauchy stresses. Fig. 6 includes corresponding FE results for isotropic distributions of rigid spherical particles. No distinction is made here of whether the particles are of the same or of different sizes since, somewhat remarkably, both classes of microstructures exhibit essentially the same large-deformation response. This is consistent with the linear elastic results of Fig. 5, where the monodisperse and polydisperse FE simulations render practically identical effective shear moduli for concentrations below $c=0.3$.

As anticipated by remark *i* in Section 4.2, Fig. 6 shows that the overall stiffness of filled Neo-Hookean rubber increases monotonically with increasing concentration of particles for all loading conditions. Another immediate observation is that the analytical and FE results are in good qualitative and quantitative agreement, with the FE results exhibiting a slightly stiffer behavior at large deformations. This trend appears to be independent of the concentration of particles.

To further probe the connections between the analytical approximation and the FE simulations, Fig. 7 compares their elastic energies $\overline{\Psi}/\mu$, normalized by the initial shear modulus μ of the underlying Neo-Hookean matrix, as functions of the principal invariants $\overline{I}_1$ and $\overline{I}_2$. Part (a) of the figure shows $\overline{\Psi}/\mu$ for fixed values of the second invariant $\overline{I}_2=3.90$ for $c=0.15$ and $\overline{I}_2=4.70$ for $c=0.05$ as functions of $\overline{I}_1$, while part (b) shows results for fixed values of the first invariant $\overline{I}_1=3.65,3.97$ for $c=0.15$ and $\overline{I}_1=4.82,5.13$ for $c=0.05$ as functions of $\overline{I}_2$. It is recalled that the constraint of incompressibility $\overline{J}=1$ imposes a restriction on the physically allowable values of $\overline{I}_1$ and $\overline{I}_2$. Thus, for fixed $\overline{I}_2=3.90$ and 4.70 the first invariant is restricted to take values in the ranges $\overline{I}_1\in[3.65,4.34]$ and $\overline{I}_1\in[4.10,5.96]$, respectively. For fixed $\overline{I}_1=3.65,3.97,4.82$, and 5.13, the corresponding allowable values of the second invariant are $\overline{I}_2\in[3.49,3.91]$, $\overline{I}_2\in[3.69,4.46]$, $\overline{I}_2\in[4.16,6.23]$, and $\overline{I}_2\in[4.31,6.98]$. These are the ranges of values utilized in the figure.

The main observation from Fig. 7 is that the FE results are approximately linear in the first invariant $\overline{I}_1$ and independent of the second invariant $\overline{I}_2$. This behavior is in accordance with that of the analytical approximation, corroborating that both results are very much identical in their functional form. The fact that the macroscopic behavior of filled Neo-Hookean rubber is functionally the same — i.e., linear in $\overline{I}_1$ and independent of $\overline{I}_2$ — as that of its underlying Neo-Hookean matrix is of note. Indeed, the functional character of the average behavior of nonlinear material systems is in general substantially different from that of its constituents, but that is not the case here.

6.3. Results for a filled silicone rubber

Finally, Fig. 8 presents various results for the large-deformation response of a filled non-Gaussian rubber, wherein the underlying matrix material is a typical silicone rubber characterized here by the stored-energy function (67) with

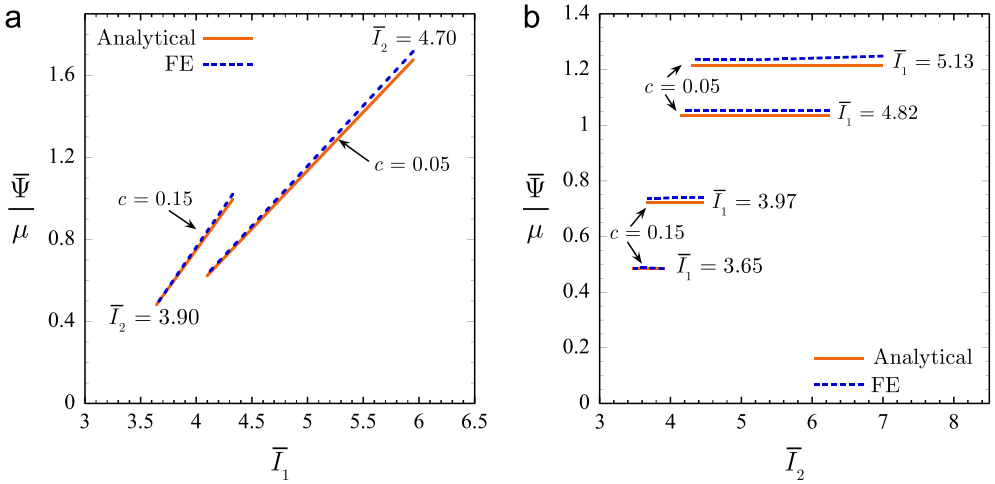

Fig. 7. Comparison of the analytical stored-energy function (56) for filled Neo-Hookean rubber with corresponding FE simulations for isotropic distributions of spherical particles. The results are shown in terms of the principal invariants $\overline{I}_1$ and $\overline{I}_2$ for two values of concentration of particles. Part (a) shows results for fixed values of $\overline{I}_2$ as functions of $\overline{I}_1$, while part (b) shows results for fixed values of $\overline{I}_1$ as functions of $\overline{I}_2$.

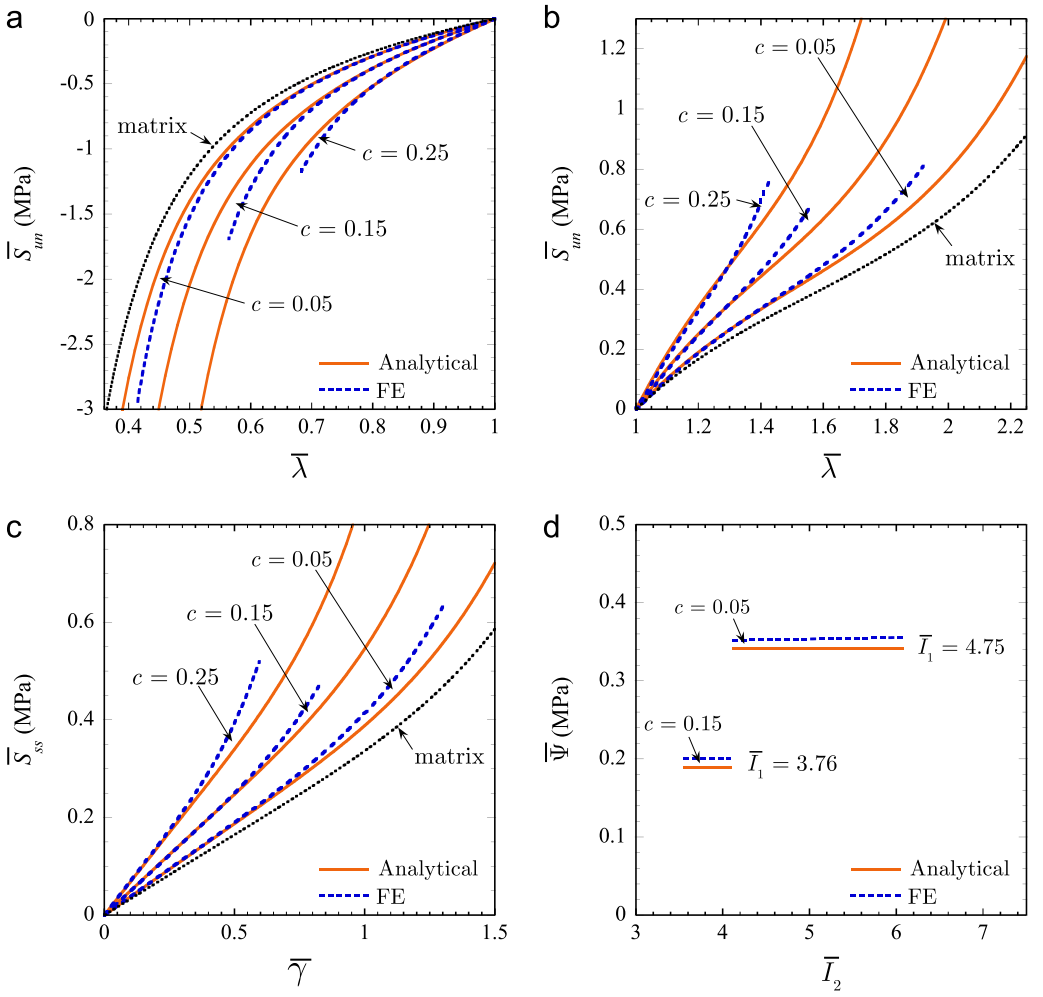

Fig. 8. Macroscopic response of filled silicone rubber with various values of concentration of particles c under: (a) uniaxial compressive, (b) uniaxial tensile, and (c) simple shear loading conditions. Plots are shown for the analytical stress-deformation results (72) and (73), and corresponding FE simulations for isotropic distributions of spherical particles. Part (d) of the figure shows comparisons between the analytical stored-energy function (71) and corresponding FE results for two fixed values of the first principal invariant $\overline{I}_1$ and c, in terms of the second invariant $\overline{I}_2$.

material parameters $\mu_1 = 0.032$ MPa, $\mu_2 = 0.3$ MPa, $\alpha_1 = 3.837$, $\alpha_2 = 0.559$. The analytical approximation (49) specializes in this case to

$$\overline{\Psi}(\overline{I}_1,\overline{I}_2,c) = (1-c)\sum_{r=1}^{2}\frac{3^{1-\alpha_r}}{2\alpha_r}\mu_r\left[\left(\frac{\overline{I}_1-3}{(1-c)^{7/2}}+3\right)^{\alpha_r}-3^{\alpha_r}\right]. \tag{71}$$

Parts (a), (b), and (c) of the figure show stress-deformation results for uniaxial compression, uniaxial tension, and simple shear for particle concentrations $c = 0.05, 0.15$, and 0.25. The constitutive stress-deformation relations for these loading conditions are given explicitly by

- *Uniaxial loading* ($\overline{\lambda}_1 = \overline{\lambda}$, $\overline{\lambda}_2 = \overline{\lambda}_3 = \overline{\lambda}^{-1/2}$ with $\overline{t}_2 = \overline{t}_3 = 0$):

$$\overline{S}_{un} = \overline{\lambda}^{-1}\overline{t}_1 = \frac{\mathrm{d}\overline{\Psi}}{\mathrm{d}\overline{\lambda}} = \frac{\overline{\lambda}-\overline{\lambda}^{-2}}{(1-c)^{5/2}}\sum_{r=1}^{2}3^{1-\alpha_r}\mu_r\left[\frac{\overline{\lambda}^2+2\overline{\lambda}^{-1}-3}{(1-c)^{7/2}}+3\right]^{\alpha_r-1} \tag{72}$$

- *Simple shear* ($\overline{\lambda}_1 = (\overline{\gamma}+\sqrt{\overline{\gamma}^2+4})/2$, $\overline{\lambda}_2 = \overline{\lambda}_1^{-1}$, $\overline{\lambda}_3 = 1$):

$$\overline{S}_{ss} = \frac{\mathrm{d}\overline{\Psi}}{\mathrm{d}\overline{\gamma}} = \frac{\overline{\gamma}}{(1-c)^{5/2}}\sum_{r=1}^{2}3^{1-\alpha_r}\mu_r\left[\frac{\overline{\gamma}^2}{(1-c)^{7/2}}+3\right]^{\alpha_r-1}, \tag{73}$$

where, again, $\overline{S}_{un}$, $\overline{S}_{ss}$ denote first Piola–Kirchhoff stress measures and $\overline{t}_1$, $\overline{t}_2$, $\overline{t}_3$ stand for the macroscopic principal Cauchy stresses. Part (d) displays results for the effective stored-energy function (71) for fixed values of the first principal invariant $\overline{I}_1=3.76$ for $c=0.15$ and $\overline{I}_1=4.75$ for $c=0.05$, in terms of the second invariant $\overline{I}_2$. All four parts of the figure include corresponding FE results for isotropic distributions of spherical particles. Akin to the preceding Neo-Hookean case, we make no distinction here of whether the particles are of the same or of different sizes since, again, the simulated monodisperse and polydisperse microstructures turn out to exhibit practically the same response for particle concentrations below $c=0.3$.

In addition to the monotonic stiffening of the response for increasing values of particle concentration, it is immediate from parts (a) through (c) of Fig. 8 that the analytical and FE results are in fairly good qualitative and quantitative agreement for all loading conditions, especially for small and moderate deformations. For large enough deformations at which the limiting chain extensibility of the silicone rubber comes into effect, the analytical results are consistently softer—as expected from their variational construction process (see remark v in Section 4.2)—than their FE counterparts. Part (d) of the figure shows that the FE results for filled silicone rubber, much like those for filled Neo-Hookean rubber, are approximately independent of the second macroscopic invariant $\overline{I}_2$, in functional accord with the analytical approximation (71).

The above three sets of sample results indicate that the analytical approximation (49) provides a mathematically simple, functionally sound, and quantitatively fairly accurate result for the overall nonlinear elastic response of non-Gaussian elastomers reinforced by isotropic distributions of rigid spherical particles of polydisperse sizes. The results have also served to reveal that size dispersion of the underlying reinforcing particles is inconsequential, in that it does not affect the overall response of the material, for particle concentrations up to the relatively high value of about $c=0.3$. Accordingly, the analytical approximation (49) can additionally be utilized to describe the response of non-Gaussian elastomers filled with isotropic distributions of spherical particles of the same size with small-to-moderate concentrations.

7. Final comments

In addition to the "hydrodynamic" reinforcement investigated in this work, it is by now well established that the presence of bound and occluded rubber contributes significantly to the overall stiffness of filled elastomers (see, e.g., Leblanc, 2010). As schematically depicted in Fig. 9(a), bound rubber refers to the interphasial material surrounding the fillers. It is typically several tens of nanometers in width, constitutively heterogeneous, and markedly stiffer than the elastomeric matrix in the bulk (see, e.g., Ramier, 2004; Qu et al., 2011). On the other hand, occluded rubber refers to the regions of matrix material that are entrapped by the agglomeration of filler particles (see Fig. 9(a)). Because of their shielding from the continuous part of the matrix, regions of occluded rubber are suspected to behave as though they were fillers (see, e.g., Heinrich et al., 2002; Leblanc, 2010). Very little attention has been paid to the incorporation of these two mechanisms into the microscopic modeling of filled elastomers, especially at large deformations. It would therefore be of great theoretical and practical value to extend the framework presented in this paper to account for such effects. The recent work of Bertoldi and Lopez-Pamies (2012) may be relevant here.

Recent experimental studies have revealed (see, e.g., Chapter 6 in Carpi et al., 2008; Danas et al., 2012) that anisotropic distributions of fillers — such as for instance the chain-like distributions shown in Fig. 9(b) — may serve to enhance certain multifunctional properties of filled elastomers, including their electro- and magneto-striction capabilities. A further practical extension of the formulation presented in this work would be to account for such anisotropic microstructures.

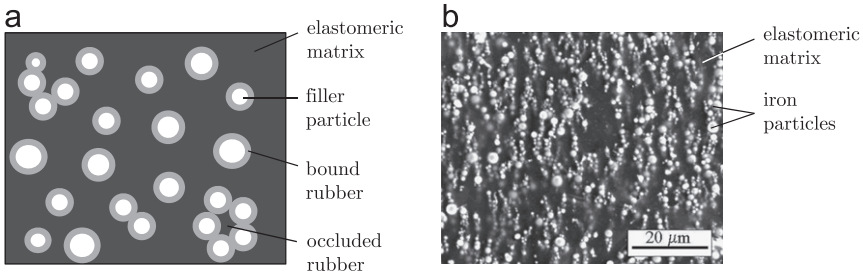

Fig. 9. (a) Schematic of bound and occluded rubber in a filled elastomer. (b) Electron micrograph of a magnetorheological elastomer with iron particles distributed anisotropically in chain-like structures (Danas et al., 2012).

Acknowledgements

Support for this work by the National Science Foundation through the CAREER Grant CMMI–1219336 is gratefully acknowledged. K.D. would also like to thank the CEE Department at UIUC for its hospitality and partial support during his visit.

References

ABAQUS Version 6.11 Documentation, Dassault Systèmes Simulia Corp., Providence, RI, USA, 2011.

Arruda, E.M., Boyce, M.C., 1993. A three-dimensional constitutive model for the large stretch behavior of rubber elastic materials. J. Mech. Phys. Solids 41, 389–412.

Avellaneda, M., 1987. Iterated homogenization, differential effective medium theory and applications. Commun. Pure Appl. Math. 40, 527–554.

Beatty, M.F., 2003. An average-stretch full-network model for rubber elasticity. J. Elasticity 70, 65–86.

Bertoldi, K., Lopez-Pamies, O., 2012. Some remarks on the effect of interphases on the mechanical response and stability of fiber-reinforced elastomers. J. Appl. Mech. 79, 031023.

Braides, A., Lukkassen, D., 2000. Iterated homogenization, differential effective medium theory and applications. Math. Models Methods Appl. Sci. 10, 47–71.

Bruggeman, D.A.G., 1935. Berechnung verschiedener physikalischer Konstanten von heterogenen Substanzen. I. Dielektrizitätskonstanten und Leitfähigkeiten der Mischkörper aus isotropen Substanzen. [Calculation of various physical constants in heterogeneous substances. I. Dielectric constants and conductivity of composites from isotropic substances]. Ann. Phys. 416, 636–664.

Carpi, F., De Rossi, D., Kornbluh, R., Pelrine, R., Sommer-Larsen, P., 2008. Dielectric Elastomers as Electromechanical Transducers. Elsevier.

Dacorogna, B., 2008. Direct Methods in the Calculus of Variations. Springer.

Danas, K., Kankanala, S.V., Triantafyllidis, N., 2012. Experiments and modeling of iron-particle-filled magnetorheological elastomers. J. Mech. Phys. Solids 60, 120–138.

deBotton, G., Shmuel, G., 2010. A new variational estimate for the effective response of hyperelastic composites. J. Mech. Phys. Solids 58, 466–483.

Fritzen, F., Forest, S., Böhlke, T., Kondo, D., Kanit, T., 2012. Computational homogenization of elasto-plastic porous metals. Int. J. Plasticity 29, 102–119.

Galli, M., Botsis, J., Janczak-Rusch, J., 2008. An elastoplastic three-dimensional homogenization model for particle reinforced composites. Comput. Mater. Sci. 41, 312–321.

Gent, A.N., 1996. A new constitutive relation for rubber. Rubber Chem. Technol. 69, 59–61.

Gusev, A.A., 1997. Representative volume element size for elastic composites: a numerical study. J. Mech. Phys. Solids 45, 1449–1459.

Hashin, Z., Shtrikman, S., 1961. Note on a variational approach to the theory of composite elastic materials. J. Franklin Inst. 271, 336–341.

Hashin, Z., Shtrikman, S., 1962. On some variational principles in anisotropic and nonhomogeneous elasticity. J. Mech. Phys. Solids 10, 335–342.

Heinrich, G., Klüppel, M., Vilgis, T.A., 2002. Reinforcement of elastomers. Curr. Opinion Solid State Mater. Sci. 6, 195–203.

Hill, R., 1972. On constitutive macrovariables for heterogeneous solids at finite strain. Proc. R. Soc. London. A 326, 131–147.

Lahellec, N., Mazerolle, F., Michel, J.-C., 2004. Second-order estimate of the macroscopic behavior of periodic hyperelastic composites: theory and experimental validation. J. Mech. Phys. Solids 52, 27–49.

Leblanc, J.L., 2010. Filled Polymers: Science and Industrial Applications. CRC Press.

Lopez-Pamies, O., 2008. Linear comparison estimates for the finite deformation of hyperelastic solids reinforced by ellipsoidal particles. Unpublished work.

Lopez-Pamies, O., 2010a. An exact result for the macroscopic response of particle-reinforced Neo-Hookean solids. J. Appl. Mech. 77, 021016.

Lopez-Pamies, O., 2010b. A new I_1-based hyperelastic model for rubber elastic materials. C. R. Mec. 338, 3–11.

Lopez-Pamies, O., Ponte Castañeda, P., 2006. On the overall behavior, microstructure evolution, and macroscopic stability in reinforced rubbers at large deformations. I. Theory J. Mech. Phys. Solids 54, 807–830.

Lopez-Pamies, O., Idiart, M.I., Nakamura, T., 2011. Cavitation in elastomeric solids: I — a defect-growth theory. J. Mech. Phys. Solids 59, 1464–1487.

Lopez-Pamies, O., Goudarzi, T., Nakamura, T. The nonlinear elastic response of suspensions of rigid inclusions in rubber: I — an exact result for dilute suspensions. J. Mech. Phys. Solids, http://dx.doi.org/10.1016/j.jmps.2012.08.010, in press.

Michel, J.C., Moulinec, H., Suquet, P., 1999. Effective properties of composite materials with periodic microstructure: a computational approach. Comput. Methods Appl. Mech. Eng. 172, 109–143.

Michel, J.C., Lopez-Pamies, O., Ponte Castañeda, P., Triantafyllidis, N., 2010. Microscopic and macroscopic instabilities in finitely strained fiber-reinforced elastomers. J. Mech. Phys. Solids 58, 1776–1803.

Milton, G.W., 2002. The Theory of Composites. Cambridge Monographs on Applied and Computational Mathematics, vol. 6. Cambridge University Press, Cambridge.

Moraleda, J., Segurado, J., Llorca, J., 2009. Finite deformation of incompressible fiber-reinforced elastomers: a computational micromechanics approach. J. Mech. Phys. Solids 57, 1596–1613.

Mullins, L., Tobin, N.R., 1965. Stress softening in rubber vulcanizates. Part I. Use of a strain amplification factor to describe the elastic behavior of filler-reinforced vulcanized rubber. J. Appl. Polym. Sci. 9, 2993–3009.

Norris, A.N., 1985. A differential scheme for the effective moduli of composites. Mech. Mater. 4, 1–16.

Ponte Castañeda, P., 1989. The overall constitutive behavior of nonlinearly elastic composites. Proc. R. Soc. London A 422, 147–171.

Ponte Castañeda, P., 1991. The effective mechanical properties of nonlinear isotropic composites. J. Mech. Phys. Solids 39, 45–71.

Ponte Castañeda, P., Tiberio, E., 2000. A second-order homogenization procedure in finite elasticity and applications to black-filled elastomers. J. Mech. Phys. Solids 48, 1389–1411.

Qu, M., Deng, F., Kalkhoran, S.M., Gouldstone, A., Robisson, A., Van Vliet, K.J., 2011. Nanoscale visualization and multiscale mechanical implications of bound rubber interphases in rubber–carbon black nanocomposites. Soft Matter 7, 1066–1077.

Ramier, J., 2004. Comportement mécanique d'élastomérs chargés, influence de l'adhésion charge–polymére, influence de la morphologie. Ph.D. Dissertation, Institut National des Science Appliquées de Lyon, France.

Roscoe, R., 1973. Isotropic composites with elastic or viscoelastic phases: general bounds for the moduli and solutions for special geometries. Rheol. Acta 12, 404–411.

Schöberl, J., 1997. Netgen an advancing front 2d/3d-mesh generator based on abstract rules. Comput. Visual. Sci. 1, 41–52.

Segurado, J., Llorca, J., 2002. A numerical approximation to the elastic properties of sphere-reinforced composites. J. Mech. Phys. Solids 50, 2107–2121.

Smallwood, H.M., 1944. Limiting law of the reinforcement of rubber. J. Appl. Phys. 15, 758–766.

Talbot, D.R.S., Willis, J.R., 1985. Variational principles for inhomogeneous nonlinear media. IMA J. Appl. Math. 35, 39–54.

Talbot, D.R.S., Willis, J.R., 1994. Upper and lower bounds for the overall properties of a nonlinear composite dielectric. I. Random microgeometry. Proc. R. Soc. London A 447, 365–384.

Torquato, S., 2002. Random Heterogeneous Materials: Micorstructures and Macroscopic Properties. Springer.

Triantafyllidis, N., Nestorvic, M.D., Schraad, M.W., 2007. Failure surfaces for finitely strained two-phase periodic solids under general in-plane loading. J. Appl. Mech. 73, 505–515.

Willis, J.R., 1983. The overall elastic response of composite materials. J. Appl. Mech. 50, 1202–1209.

Willis, J.R., 1991. On methods for bounding the overall properties of nonlinear composites. J. Mech. Phys. Solids 39, 73–86.

Willis, J.R., 1994. Upper and lower bounds for the properties of nonlinear composites. Mater. Sci. Eng. A 175, 7–14.

Willis, J.R., 2002. Mechanics of Composites. Lecture Notes. University of Cambridge, Cambridge, UK.

Zee, L., Sternberg, E., 1983. Ordinary and strong ellipticity in the equilibrium theory of incompressible hyperelastic solids. Arch. Ration. Mech. Anal. 83, 53–90.